

**Assessment of BISON:
A Nuclear Fuel Performance Analysis Code**

D. M. Perez, R. L. Williamson, S. R. Novascone,
G. Pastore, J. D. Hales, B. W. Spencer

Fuels Modeling & Simulation Department
Idaho National Laboratory
Idaho Falls, ID

November 2013

Abstract

A high-level summary of an effort to assess the predictive capability of BISON, a nuclear fuel performance code, is presented. This assessment was focused mainly on LWR fuel, and to a lesser degree, TRISO particle fuel. A comparison of BISON simulation results to a variety of experimental measurements of instrumented LWR fuel rods are shown. The source of LWR experimental data is primarily from the IAEA's FUMEX program. Benchmark simulation results of TRISO-coated particles are compared to BISON simulations. The TRISO benchmark simulations originate from the IAEA Coordinated Research Program. A brief discussion of material models and modeling approaches is also presented. There was a concerted effort to avoid model tuning to a particular set of experimental measurements. The material models and approaches were reviewed by the BISON team, and a subset of these were used for all the BISON simulations. As such, the BISON results shown in this assessment document are best-estimate as of fall 2013.

Overall, BISON simulations compare quite well with LWR experimental measurements and benchmark TRISO simulations. Discussion of future development and assessment efforts are also presented. More detailed versions of each assessment case are documented and can be found at the INL BISON repository.

Contents

1. Introduction	4
2. Light Water Reactor Fuel	5
2.1. Assessment Cases	5
2.2. Material and Behavioral Models	5
2.3. Thermal Behavior	7
2.3.1. Beginning of Life	7
2.3.2. Through Life	8
2.3.3. Ramp Tests	8
2.3.4. Thermal Behavior Summary	9
2.4. Fission Gas Behavior	9
2.4.1. Fission Gas Behavior Summary	11
2.5. Mechanical Behavior	11
2.5.1. Clad Elongation	11
2.5.2. Clad Final Diameter	12
2.5.3. Mechanical Behavior Summary	14
3. TRISO-Coated Particle Fuel	15
3.1. Assessment Cases	15
3.2. Results	16
3.3. Summary	20
Appendices	22
A. IFA 431 Rods 1, 2, and 3	22
B. IFA 432 Rods 1, 2, and 3	28
C. IFA 515.10 Rod A1	34
D. IFA 597.3 Rods 7 and 8	39
E. Risø AN3	47
F. AREVA Idealized Case	53
G. FUMEX-II Simplified Cases	59
H. Risø GE7	71
I. OSIRIS J12	78
J. REGATE	84

1. Introduction

BISON is a modern finite-element based nuclear fuel performance code that has been under development at the Idaho National Laboratory since 2009 [1]. The code is applicable to both steady and transient fuel behavior and can be used to analyze either 1D spherical, 2D axisymmetric or 3D geometries. BISON has been applied to a variety of fuel forms including Light Water Reactor (LWR) fuel rods [1], TRISO-coated particle fuel [2], and metallic fuel in both rod [3] and plate geometries.

From the beginning, the development of BISON and related software has been accompanied by the creation of numerous verification tests in which specific features of the code are tested to see if they compute the correct analytical or known solution. There are currently over 800 of these regression tests for the MOOSE/ELK/FOX/BISON code hierarchy. During code development, the tests are run frequently (typically several times a day) and the solutions checked on a variety of computer platforms.

In addition, efforts have begun to assess BISON's ability to predict fuel behavior by comparison to data from a variety of instrumented LWR fuel rods and by code comparison for a series of TRISO-coated particle fuel benchmark cases. This assessment effort has been invaluable, leading to the discovery of development oversights not apparent from the simpler regression tests. Additionally it has led to improved confidence in BISON's ability to predict nuclear fuel behavior.

To date, 19 integral LWR fuel rod assessment cases, which include comparisons to 23 measurements, have been completed. These cases were selected to assess the code's ability to simulate a variety of physical behaviors including thermal response both early in life and during power ramping, fission gas release, and mechanical behavior including both cladding elongation and pellet clad mechanical interaction (PCMI). Many of these assessment cases grew out of participation in the International Atomic Energy Agency (IAEA) sponsored FUMEX-III Coordinated Research Project [4] and are priority cases from either FUMEX-II [5] or FUMEX-III. Other cases were chosen based on recommendations from nuclear fuel experts.

For TRISO-coated particle fuel, a set of 13 benchmark cases have been considered which compare BISON results to those from other fuel performance codes, under normal operation and operational transients. These cases originated as part of an IAEA Coordinated Research Program (CRP-6) on High Temperature Gas Reactor (HTGR) fuel [6].

Chapters 2 and 3 summarize the LWR and TRISO cases, respectively. Each LWR assessment case is discussed in further detail in the attached appendices. Each result reported here-in is based on BISON 1.0 and ran on a MacPro workstation. All cases can also be run on the INL high performance computer FISSION.

2. Light Water Reactor Fuel

2.1. Assessment Cases

As summarized in Table 2.1, 19 integral fuel rod LWR assessment cases have been simulated, including 23 comparisons to measurement. Indicated in the table are the measured quantities for comparison, namely fuel centerline temperature (FCT) at beginning of life (BOL), throughout life (TL), and during power ramps (Ramps), fission gas release (FGR), cladding elongation (Clad-Elong), and cladding outer diameter following pellet clad mechanical interaction (PCMI).

Table 2.1.: Summary table of BISON LWR assessment cases.

Experiment	Rod	FCT BOL	FCT TL	FCT Ramps	FGR	Clad-Elong	Clad-Dia (PCMI)
IFA-431	1	X					
IFA-431	2	X					
IFA-431	3	X					
IFA-432	1	X					
IFA-432	2	X					
IFA-432	3	X					
IFA-515.10	A1	X					
IFA-597.3	7			X		X	
IFA-597.3	8			X			
Risø-3	AN3			X	X		
AREVA Idealized Case					X		
FUMEX-II	27(1)				X		
FUMEX-II	27(2a)				X		
FUMEX-II	27(2b)				X		
FUMEX-II	27(2c)				X		
FUMEX-II	27(2d)				X		
Risø-3	GE7				X		X
OSIRIS	J12						X
REGATE					X		X

2.2. Material and Behavioral Models

This section briefly reviews the BISON material and behavior models used in analyzing the LWR assessment cases. Theoretical details may be found in the BISON Theory Manual [7], and descriptions of the input options for the models are in the BISON User's Manual [8].

Burnup Evolution of burnup is typically driven by a table of rod averaged linear power at given times in the analysis. Axial variations are described in a similar manner. The radial power profile is modeled according to [9]. Given the local power, the local fission rate may be computed, and the fission rate is directly related to the evolving burnup. (See [7, Power, Burnup, and Related Models][8, Burnup].)

Contact Mechanical contact is enforced using node/face constraints. The penalty algorithm is commonly used. The interaction is enforced with a frictionless model. (See [7, Mechanical Contact][8, Mechanical Contact].)

Elastic An elastic material law is used for the fuel. A creep model is available but was not chosen due to the fact that it predicts excessive creep as a result of excessively high stresses in the absence of a cracking model. Typical parameters are 2×10^{11} N/m² for Young's modulus and 0.345 for Poisson's ratio. The coefficient of thermal expansion is 10×10^{-6} m/m/K. (See [8, Solid Mechanics Models].)

GrainRadiusAux When a polycrystalline material is subject to high temperatures, larger grains tend to grow at the expense of the smaller ones. As a consequence, the latter gradually disappear, thus reducing the total number of grains per unit volume and increasing the average grain size. The granular structure of the fuel affects physical processes such as fission gas behavior (Section 2.4). A simple empirical model [10] is implemented in BISON for calculating grain growth in UO₂ fuel. (See [7, Grain Growth][8, Other AuxKernels].)

HeatConductionMaterial The general HeatConductionMaterial is used to set the thermal conductivity and specific heat for the clad. Thermal conductivity is set at 16 W/m/K, and specific heat is 330 J/kg/K. (See [8, Thermal Models].)

IrradiationGrowthZr4 The IrradiationGrowthZr4 model incorporates anisotropic volumetric swelling to track axial elongation in Zr4 cladding. The model is taken from ESCORE [11]. (See [7, Irradiation Growth][8, Solid Mechanics Models].)

MechZry The MechZry model is capable of tracking primary, thermal, and irradiation-induced creep in clad. Typical parameters are 7.5×10^{10} N/m² for Young's modulus and 0.3 for Poisson's ratio. The coefficient of thermal expansion is 5×10^{-6} m/m/K. (See [7, Thermal and Irradiation Creep; Limbäck Creep Model][8, Solid Mechanics Models].)

RelocationUO2 RelocationUO2 accounts for cracking and relocation of fuel pellet fragments in the radial direction. This model is necessary for accurate modeling of LWR fuel. (See [7, Relocation][8, Solid Mechanics Models].)

Sifgrs The Simple Integrated Fission Gas Release and Swelling (Sifgrs) model is intended for consistently evaluating the kinetics of both fission gas swelling and release in UO₂. (See [7, Fission Gas Behavior][8, Fission Gas Models].)

ThermalContact The transfer of heat from the fuel to the cladding is accomplished via the ThermalContact model. The model is based on [12]. This model includes a computation of the conductivity of the gas using the MATPRO model [13], increased conductance due to mechanical contact [12], and radiant heat transfer. Temperature jump distance is computed [14]. Typical roughness values are 1 μ m for the clad and 2 μ m for the fuel, with a roughness coefficient of 3.2. (See [7, Gap Heat Transfer][8, Thermal Contact].)

ThermalFuel The ThermalFuel model incorporates several empirical fits for thermal conductivity of UO₂. The assessment cases were run with the NFIR correlation [15]. The NFIR model contains a temperature dependent thermal recovery function that accounts for self-annealing of defects in the fuel as it heats up. The ultimate effect of the self-annealing is a slight increase of the thermal conductivity over a range of temperatures up to ~ 1200 K. (See [7, Thermal Properties][8, Thermal Models].)

VSwellingUO2 The VSwellingUO2 model computes a volumetric strain to account for solid and gaseous swelling and densification. (See [7, Fission Product Swelling; Densification][8, Solid Mechanics Models].)

2.3. Thermal Behavior

The ability to accurately predict fuel rod thermal behavior is essential for fuel performance analysis. Temperatures drive many other important physical phenomena, such as fission gas release and clad thermal creep. Peak fuel temperatures are of primary importance in determining fuel rod performance and lifetime.

2.3.1. Beginning of Life

Seven of the rods simulated to date considered only the first rise to power, also referred to as beginning of life (BOL). Temperature comparisons during the first rise to power are significant as they isolate several important aspects of fuel rod behavior before complexities associated with higher burnups are encountered. Proper prediction of BOL centerline temperatures requires accurate models for the fuel and clad thermal conductivity, gap heat transfer, thermal expansion of both the fuel and the clad materials (to predict an accurate gap width), and fuel relocation. Figure 2.1 summarizes the BOL fuel centerline temperature comparisons for all cases considered. Plotted is the measured versus predicted temperature as the rod power is increased during power-up. The solid line indicates a perfect comparison, and the dashed lines indicate ± 10 percent error. For all BOL cases considered to date, BISON does a good job of predicting the fuel centerline temperature.

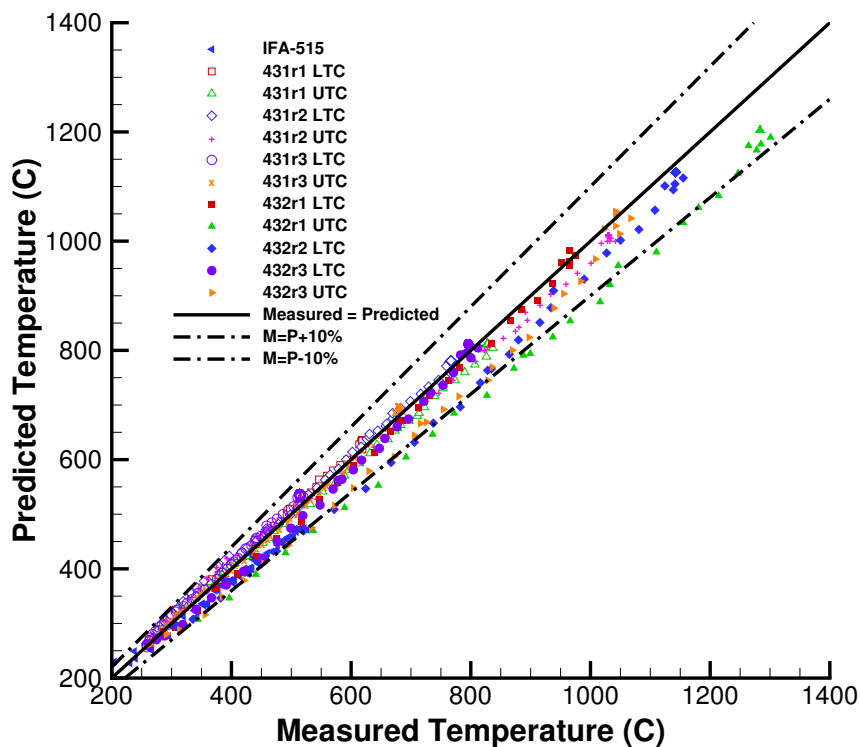


Figure 2.1.: BOL measured vs. predicted fuel centerline temperature for rods 1, 2, and 3 in IFA-431, IFA-432, and IFA-515.10 Rod A1. LTC and UTC stand for lower and upper thermocouple measurements, respectively.

2.3.2. Through Life

Currently no through-life assessment cases are sufficiently complete to report. The cases that have been used for BOL comparisons could be run through the entire irradiation history to get through life comparisons. The HALDEN power history is very complex with data given every 900 seconds. Further work is required with the raw power data received from HALDEN to condense the data set before through life comparisons can be made.

2.3.3. Ramp Tests

Three ramp test rods have been completed to date: Risø AN3, IFA-597.3 rod 7 and rod 8. Rods 7 and 8 in the IFA-597 series were run in the same simulation as they are identical rods. These two rods are considered as one result, where the experimental data from rod 7 is used in the clad elongation comparisons (see Section 2.5) and experimental data from rod 8 is used in the fuel centerline temperature (FCT) and fission gas release (FGR) comparisons (for FGR comparisons, see Section 2.4).

Typically, ramp tests are performed on used commercial fuel rods or sections of fuel rods. To accurately predict the fuel behavior during these ramp tests, the base irradiation (commercial reactor) power history is simulated on the fuel segment followed by the test power ramp history.

BISON predicts the fuel centerline temperature well (as an example see Figure 2.2, which is the FCT comparisons for the Risø AN3 ramp test) and is comparable with other well-known fuel performance codes. The fuel centerline temperature for this particular case is taken at a node approximately 36.4 mm from the top of the fuel stack, approximately 1.5 pellet lengths from the bottom of the thermocouple hole, (black dot on mesh in Figure 2.2).

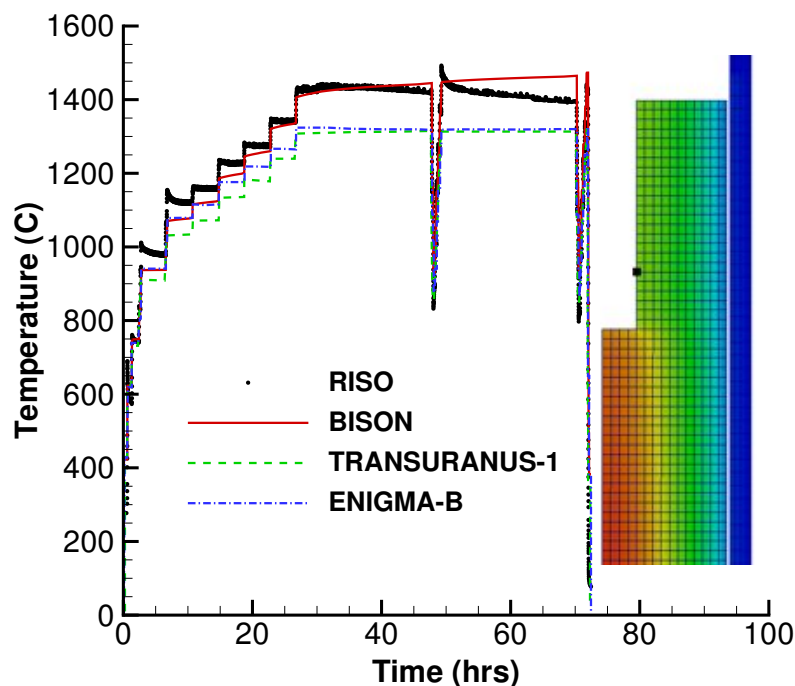


Figure 2.2.: BISON fuel centerline temperature compared to Risø AN3 experimental data and the fuel performance codes TRANSURANUS and ENIGMA. The thermocouple location is indicated on the inset temperature contour plot.

The IFA-597.3 series underwent multiple power ramps as shown in Figure D.2. The fuel centerline temperature during the first four power ramps and the last power ramp from Figure D.2 were used for

the FCT comparisons. BISON predicts the fuel centerline temperature well; however, the temperature falls slightly under the measured values, see Figure 2.3.

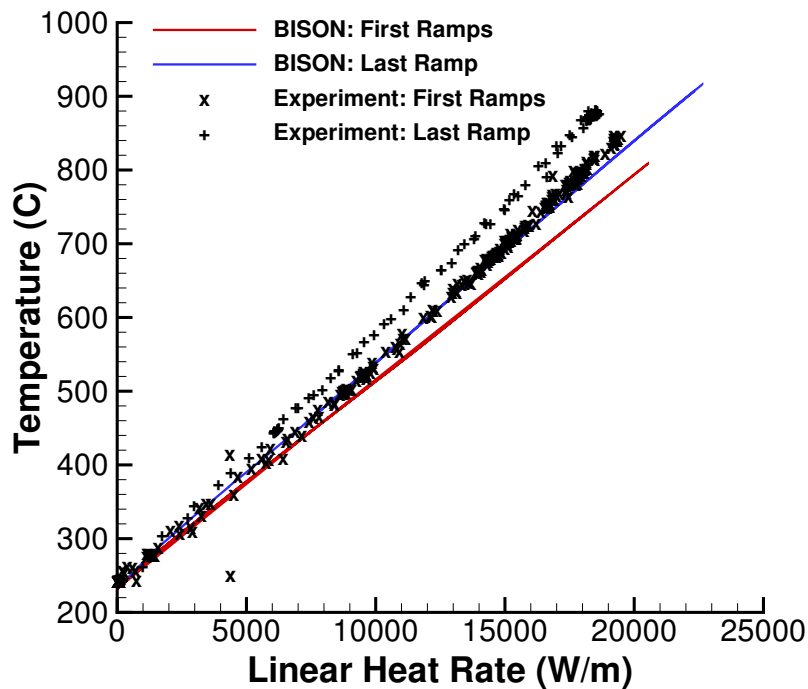


Figure 2.3.: BISON fuel centerline temperature compared to Halden IFA-597.3 experimental data.

2.3.4. Thermal Behavior Summary

BOL and ramp temperature measurements of LWR experiments were compared to BISON simulation results in order to evaluate the models used in BISON. The comparisons show the BISON calculations are reasonably close to experimental measurements. This is significant because fuel temperatures strongly affect important physical processes such as fission gas release and clad creep and directly determine fuel rod life. Topics for future work include through-life temperature comparisons plus additional priority cases from FUMEX-II and III.

2.4. Fission Gas Behavior

The processes induced by the generation of the fission gases xenon and krypton in nuclear fuel have a strong impact on the thermo-mechanical performance of the fuel rods. On the one hand, the fission gases tend to precipitate into bubbles resulting in fuel swelling, which promotes pellet-cladding gap closure and the ensuing pellet-cladding mechanical interaction (PCMI). On the other hand, fission gas release (FGR) to the fuel rod free volume causes pressure build-up and thermal conductivity degradation of the rod filling gas.

A Simple Integrated Fission Gas Release and Swelling (Sifgrs) model is available in BISON for the coupled fission gas swelling and release in UO_2 . The model is founded on a physics-based description of the relevant processes, while retaining a level of complexity consistent with the application to engineering-scale nuclear fuel analysis. The Sifgrs model draws on and extends the approach described in [16].

The mutual dependence between fission gas behavior and grain growth is taken into account in Sifgrs through coupling with the grain growth model (Section 2.2).

As a first step, the model was implemented and tested in BISON for the analysis of FGR only [17]. More recently, the calculation of the fission gas swelling as coupled with the FGR has been introduced and matched with the mechanical analysis in BISON. Testing of the full Sifgrs fission gas release and swelling model is underway. First results are presented in this report, including comparisons with the empirical fission swelling model from MATPRO [18], also available in BISON.

The Vitanza Criterion was simulated to determine the burnup dependent threshold temperature at which more than 1% FGR can be expected. BISON falls within the ranges of other well-known fuel performance codes as shown in Figure 2.4.

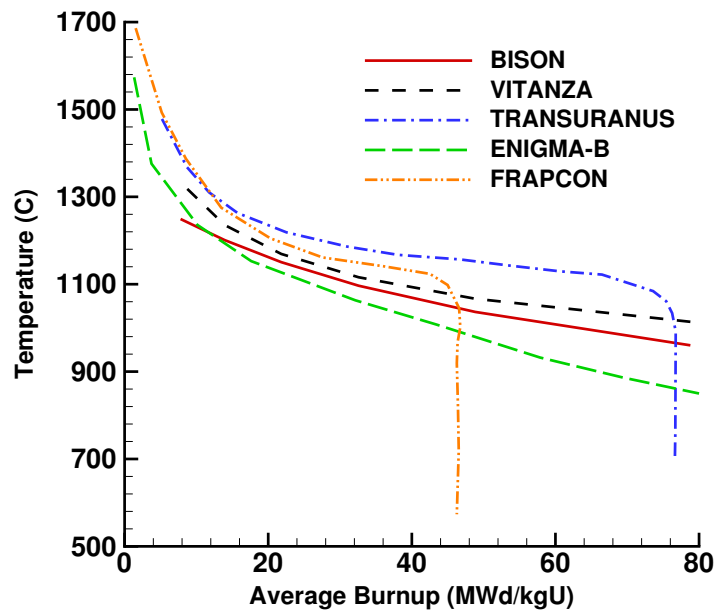


Figure 2.4.: 27(1) BISON and other code results compared to Vitanza criteria [19].

FGR comparisons were performed with multiple assessment cases (see Table 2.1). To best summarize a majority of these comparisons, a measured versus predicted plot of the end of life total fission gas release is shown in Figure 2.5.

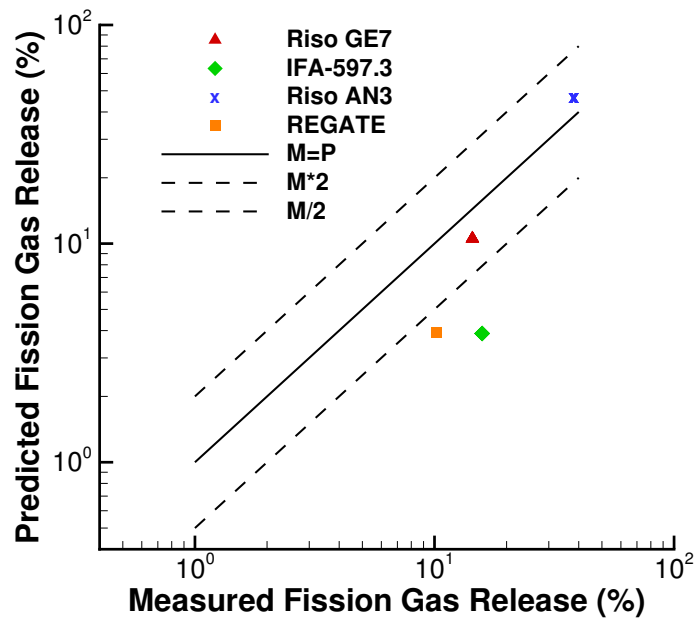


Figure 2.5.: Measured vs. predicted end of life total fission gas release comparisons.

2.4.1. Fission Gas Behavior Summary

BISON predicts the total FGR well at low burnup, however, at high burnup, BISON under predicts the total FGR. To date, the Sifgrs model provides a basis for integrating increasingly accurate descriptions of the fission gas swelling and release mechanisms. Development of the treatment of the peculiar kinetics of FGR during rapid power transients (burst release), and the more advanced description of the intra-granular gas behavior, including consideration of the fuel swelling contribution due to intra-granular gas bubbles is currently underway.

2.5. Mechanical Behavior

Accurately representing the mechanical behavior of the fuel and clad is also essential when simulating fully-coupled thermomechanics problems like LWR fuel pins. Together with the thermal solution, the mechanical models determine the fuel-clad gap size, which may be the single most important characteristic to quantify in LWR simulations. Simulating realistic mechanical behavior is also critical when attempting to make predictions about clad structural integrity during pellet clad mechanical interaction (PCMI).

The following sections summarize BISON simulations of experiments where the fuel pellets have come into contact with the clad. Measurements of final clad length and diameter are compared to BISON calculations. These comparisons showcase the fuel and clad mechanical behavior models such as thermal expansion, clad irradiation growth, clad creep, fuel relocation, fuel swelling, fuel densification, and, perhaps most importantly, the mechanical interaction of fuel and clad as the two come into contact.

2.5.1. Clad Elongation

One way to quantify the mechanical behavior of LWR fuel rods is clad elongation. The point in time at which fuel and clad interact mechanically itself depends on several factors including pellet fracturing and relocation. It is also important to recognize that the eccentric placement of fuel pellets in the clad allows mechanical interaction from very early times.

Once the mechanical interaction begins, the relative motion of the fuel and clad depends on the friction between them. The value of the friction coefficient is understood to come with a large amount of uncertainty.

One clad elongation case has been included to date: IFA-597. This case has been run with frictionless and glued (infinite friction) contact conditions to bound the solution. A plot of elongation vs. time is shown in Figure 2.6.

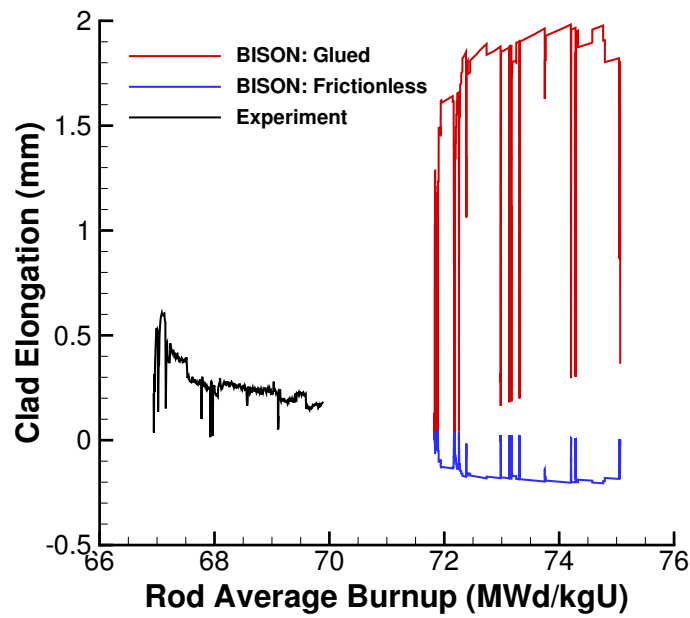


Figure 2.6.: IFA-597 elongation comparison.

2.5.2. Clad Final Diameter

Clad final diameter simulations and measurements are another way to quantify mechanical behavior models. The three experiments considered to date where final rod diameter measurements were made are Risø-3 GE7, OSIRIS J12, and REGATE. These experiments all consisted of a base irradiation followed by application of a power ramp before the end of the experiment. Final diameter measurements compared to BISON calculations of final diameter size are presented in Figures 2.7, 2.8, and 2.9.

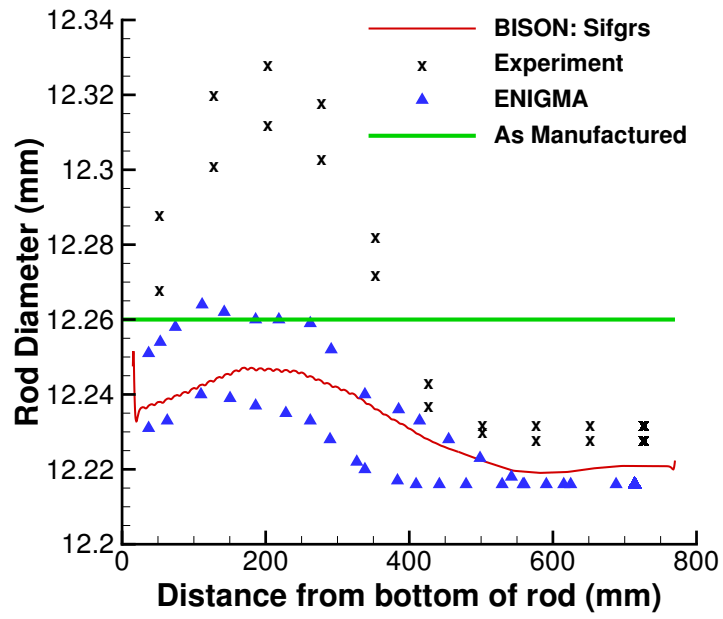


Figure 2.7.: Risø GE7 diameter comparison.

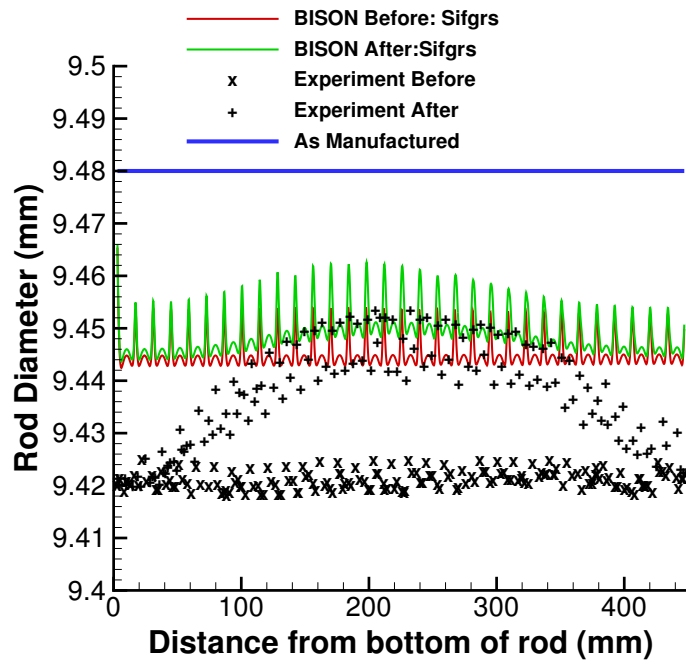


Figure 2.8.: OSIRIS J12 diameter comparison.

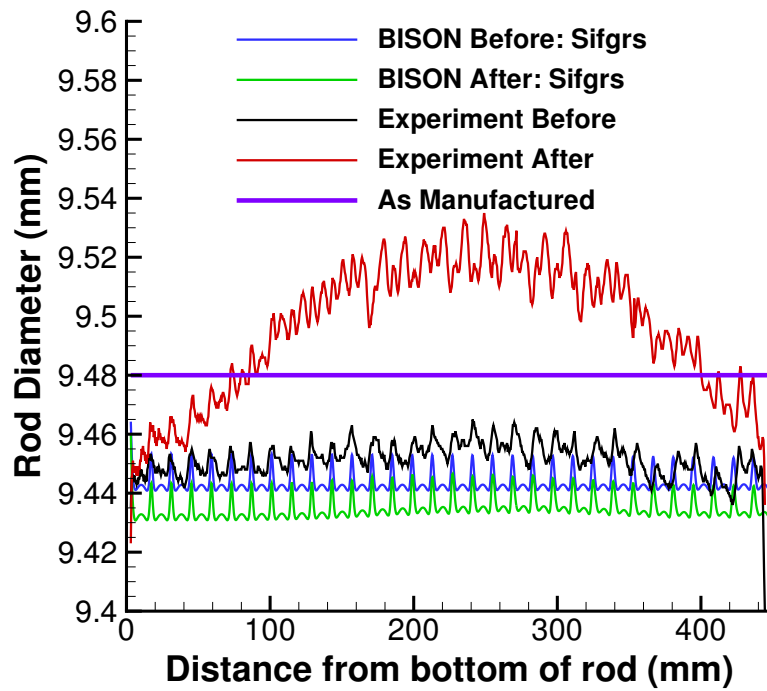


Figure 2.9.: REGATE diameter comparison.

2.5.3. Mechanical Behavior Summary

Clad elongation and final diameter experimental measurements and BISON calculations have been presented for the purpose of quantifying the mechanical behavior and contact models in BISON. Overall, the comparisons are good but show a need for more accurate models. One possibility is to upgrade the nonlinear material models. For example the clad creep models (primary, secondary, and tertiary) and instantaneous plasticity could be coupled. Perhaps more importantly, more information regarding clad material characteristics (e.g. exact alloy specifications) and testing under realistic environments (thermal and irradiated) could be obtained via testing programs and incorporated into the material models. Further development work on nonlinear material modeling is an area of focus for next year.

3. TRISO-Coated Particle Fuel

3.1. Assessment Cases

As part of an International Atomic Energy Agency (IAEA) Coordinated Research Program (CRP-6) on High Temperature Gas Reactor (HTGR) reactor fuel technology, a set of benchmarking activities were developed to compare fuel performance codes under normal operation and operational transients [6]. Sixteen benchmark cases were identified, ranging in complexity from a simple fuel kernel having a single elastic coating layer, to realistic TRISO-coated particles under a variety of irradiation conditions. In each case, the particle geometry, constitutive relations, material properties, and operating conditions were carefully prescribed to minimize differences between the various code predictions; details are given in [6]. As an early code assessment exercise, BISON has been applied to 13 of the 16 benchmark cases, as summarized in Table 3.1.

Table 3.1.: IAEA CRP-6 benchmark cases considered in the BISON coated-particle assessment exercise. HFR-K3 and HFR-P4 are German pebble and fuel element experiments, respectively.

Case	Geometry	Description
1	SiC layer	Elastic only
2	IPyC layer	Elastic only
3	IPyC/SiC	Elastic with no fluence
4a	IPyC/SiC	Swelling and no creep
4b	IPyC/SiC	Creep and no swelling
4c	IPyC/SiC	Creep and swelling
4d	IPyC/SiC	Creep- and fluence-dependent swelling
5	TRISO	350 μm kernel, real conditions
6	TRISO	500 μm kernel, real conditions
7	TRISO	Same as 6 with high BAF PyC
8	TRISO	Same as 6 with cyclic temperature
10	HFR-K3	10% FIMA, $5.3 \times 10^{-25} \text{ n/m}^2$ fluence
11	HFR-P4	14% FIMA, $7.2 \times 10^{-25} \text{ n/m}^2$ fluence

The models for all benchmark cases used either six or eight quadratic axisymmetric finite elements across the width of each coating layer. A typical mesh with eight elements per layer is shown in Figure 3.1. Note that, in addition to the axisymmetry condition, a symmetry plane is also assumed along the top of the mesh. For cases 1 and 2, numerical solutions were also obtained with twelve elements across the coating layer to determine whether the mesh was sufficiently refined. Maximum tangential stresses obtained from the refined mesh models differed at most by 0.1%, demonstrating adequate mesh convergence with the coarser meshes. Since all of the cases are spherically symmetric, identical results (within machine precision) can be obtained using either 1D spherically symmetric or 3D elements.

The BISON input and all supporting files (mesh, mesh scripts, etc.) for the thirteen TRISO benchmark cases are provided with the code distribution at `bison/assessment/TRISO_benchmarks`. For users who wish to run these benchmarks, additional explanation is required. Because the IAEA CRP cases involved comparison of results from a large number and variety of codes, the particle geometry, boundary conditions and material models were prescribed for each case in detail. This was done principally to avoid differences in material models, which can be substantial between the various codes. In some cases these prescribed models differed from the standard BISON TRISO material models. Rather than

implement these numerous and specific models in the code, temporary models were developed and the necessary source code to use these models was stored with the individual cases. For the benchmark cases requiring these models (all except 1-3), users must overwrite the material model source code, re-compile, run the problem, and revert back to the original source. Refer to README files, included in each directory where such modifications are required, for more detail. This cumbersome process will be eliminated in the future.

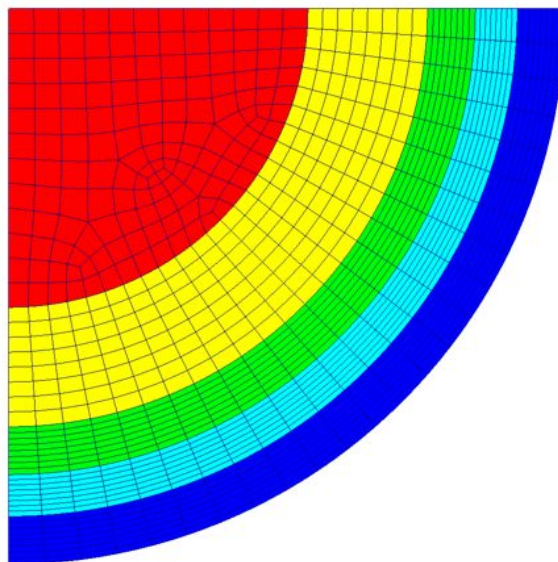


Figure 3.1.: Typical computational mesh used for the IAEA CRP-6 benchmark cases.

3.2. Results

Cases 1 to 3 were limited to single and double coating layers and tested simple elastic thermomechanical behavior against analytical solutions. A comparison of the analytical and BISON numerical solutions for the maximum tangential stress, which occurs at the inner surface of the various layers, is shown in Table 3.2. Comparisons are excellent.

Table 3.2.: Comparison of the BISON computed maximum tangential stress (MPa) to the analytical solution for Cases 1 to 3.

Case	Layer	Analytical	BISON	Error (%)
1	SiC	125.19	125.23	0.032
2	IPyC	50.200	50.287	0.173
3	IPyC/SiC	8.8/104.4	8.7/104.5	1.14/0.10

Cases 4a to 4d included both IPyC and SiC layers and investigated pyrolytic carbon layer behavior under a variety of conditions. Cases 5 to 8 considered a single TRISO particle with more complexity added with each subsequent case. For cases 1 to 4d, the internal gas pressure was fixed at 25 MPa while cases 5 to 8 included a linear pressure ramp. The particle temperature was held uniform at 1273 K for cases 1 to 7, but for case 8 was cycled ten times between 873 and 1273 K, characteristic of fuel in a pebble bed reactor. For cases 4 to 7, Table 3.3 compares BISON computed solutions to the range of solutions from eight coated-particle fuel codes included in the CRP-6 exercise [6]. Comparisons are of

the tangential stress at the inner surface of both the IPyC and SiC layers, at the end of irradiation. The BISON solutions are always within the range of values computed by the other codes. Note that tabulated values defining the ranges were extracted from plots in [6] and are thus not precise.

Table 3.3.: Comparison of the BISON computed tangential stress (MPa) to the range of values computed by the codes included in the CRP-6 exercise. Comparisons are at the inner surface of each layer and at the end of irradiation.

Case	Layer	CRP-6 codes [range]	BISON
4a	IPyC/SiC	[925, 970]/[-775, -850]	928/-819
4b	IPyC/SiC	[-25, -25]/[138, 142]	-25.0/139
4c	IPyC/SiC	[25, 27]/[83, 92]	26.0/89.4
4d	IPyC/SiC	[25, 35]/[71, 88]	27.8/87.0
5	IPyC/SiC	[40, 58]/[-56, -28]	41.9/-32.2
6	IPyC/SiC	[27, 38]/[28, 48]	29.2/44.9
7	IPyC/SiC	[37, 50]/[10, 25]	38.0/24.6

Although code comparisons in Table 3.3 are provided only at the end of irradiation, comparisons were made at various intermediate times during the irradiation period. The BISON solutions were always within the range of solutions produced by the CRP-6 codes.

Figure 3.2 compares solutions for case 8, which involved a cyclic particle temperature, during the full irradiation history. In this figure, BISON solutions of the tangential stress at the inner wall of the IPyC and SiC layers are compared to solutions from three codes from the CRP-6 exercise, namely PARFUME [20], ATLAS [21] and STRESS3 [22]. As above, data for the code comparisons were extracted from plots in [6]. For the IPyC layer, the four solutions essentially overlay each other during the entire irradiation period. In the SiC layer, the four solutions are quite similar but some differences are evident, particularly for the first four temperature cycles. The BISON solution falls roughly midway between the PARFUME and STRESS3 solutions and is essentially identical to the ATLAS solution.

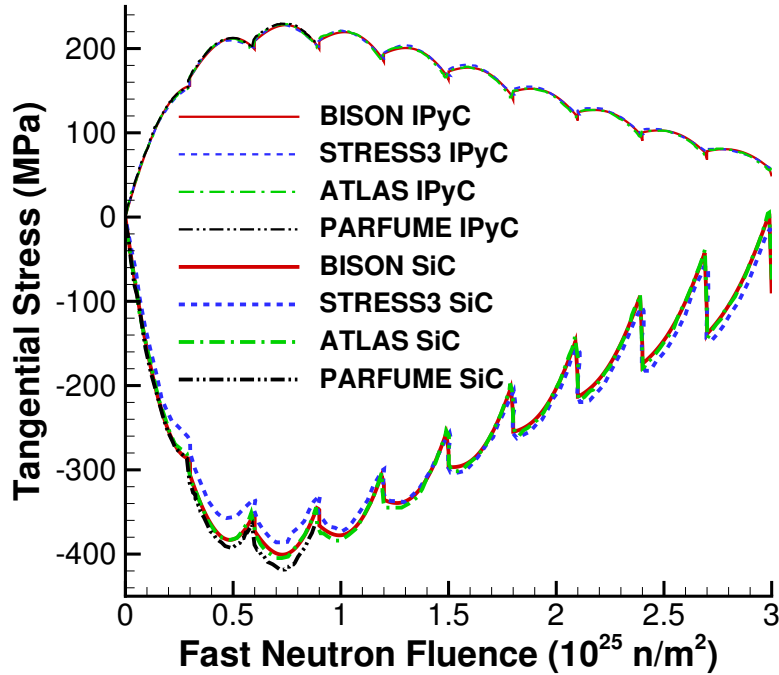
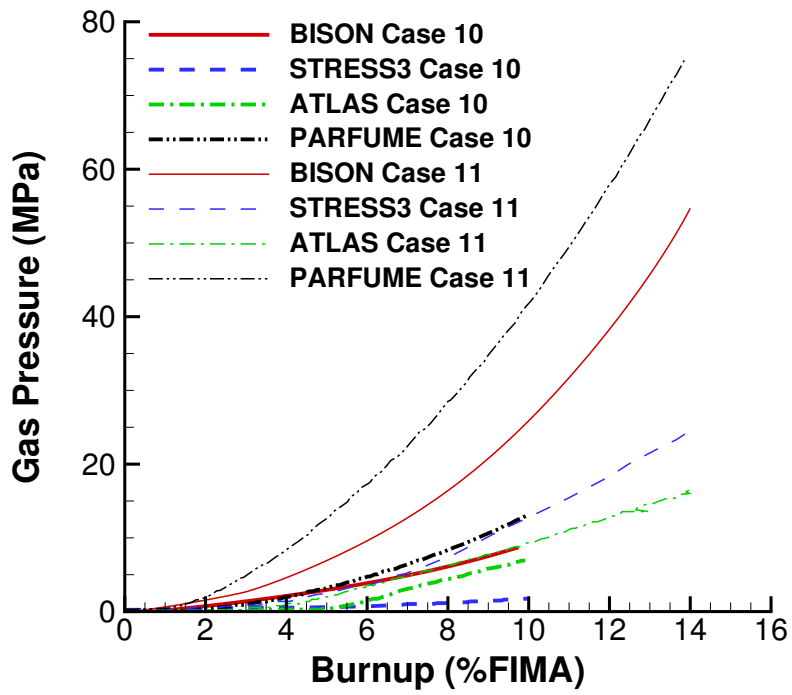


Figure 3.2.: Code comparison for case 8, which included a ten cycle temperature history. Plotted is the tangential stress at the inner wall of the IPyC and SiC layers.

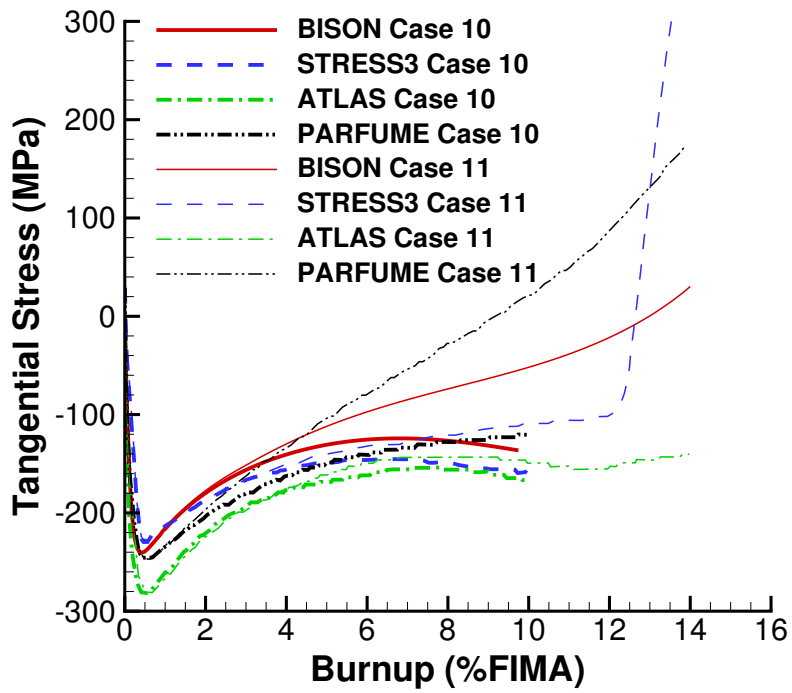
Cases 9 to 13 in CRP-6 were more complicated benchmarks based on past or planned experiments with TRISO-coated particles. The two cases considered here (10 and 11) were based on German fuel from pebble and fuel element experiments. Again, details are provided in [6]. Although material properties and constitutive relations were prescribed for these cases, they differed from cases 1 to 8 in two ways: (1) the internal pressure was not fixed but instead determined by fission gas release and CO production and (2) the particle size was prescribed as a population (mean value and standard deviation) rather than a single value. BISON solutions were based on the gas release and CO production models described above; however, for simplicity, only a single particle size was considered based on the mean particle diameter.

Figure 3.3 provides code comparisons of the total gas pressure (Figure 3.3(a)) and tangential stress at the inner wall of the SiC layer (Figure 3.3(b)) for benchmark cases 10 and 11. Again, BISON is compared to three codes from the CRP-6 exercise. Substantial differences exist in these solutions, particularly for the gas pressure. The BISON solution histories, however, compare well to the range of solutions given by the three well-established codes chosen for comparison.

As stated in [6], the differences between various code predictions shown in Figures 3.3(a) and 3.3(b) can be largely attributed to the models used to calculate fission gas release and CO production in the kernel. A detailed description of these models is not available in [6], limiting more detailed investigation. One obvious and significant difference is that both BISON and ATLAS employ the simple Proksch et al. [23] empirical model for CO production while PARFUME [20] uses a detailed thermochemical model.



(a)



(b)

Figure 3.3.: Code comparisons of the total gas pressure (a) and tangential stress at the inner wall of SiC layer (b) for benchmark cases 10 and 11.

3.3. Summary

Since the IAEA CRP cases involved comparison of results from a large number and variety of codes, the particle geometry, boundary conditions and material models were prescribed for each case in detail. This was done principally to avoid differences in material models, which can be substantial between the various codes. In some cases these prescribed models differed from the standard BISON TRISO material models. Rather than implement these numerous and specific models in the code, temporary models were developed and the necessary source code to use these models was stored with the individual cases. BISON compares well with the other codes for these benchmark cases.

It is also important to assess the TRISO material models currently within BISON against experimental results. The beginning of this assessment work is planned to occur in FY 2014.

Appendices

A. IFA 431 Rods 1, 2, and 3

A.1. Overview

The IFA-431 experiment was part of an effort by the US NRC to obtain well-characterized experimental data under conditions that simulate long-term steady LWR operation [24]. IFA-431 was a heavily instrumented fuel assembly irradiated in the Halden boiling water reactor from 1975 to 1976. The test rods initially contained fresh fuel and were operated at power levels near the upper bound for full-length commercial fuel rods.

The IFA-431 assembly included six instrumented rods, each with centerline temperature instrumentation in both the top and bottom ends of the fuel column. Three of the six rods (Rods 1, 2, 3) are the focus of this assessment.

The IFA-431 assembly also contained neutron detectors, coolant thermocouples, a coolant flow meter, and a transducer to measure internal rod pressure.

A.2. Test Description

The three test rods considered here were designed to simulate BWR-6 rod cladding material and dimensions, and included only differences in fuel-cladding gap width. The general rod specifications are summarized in Table A.1 which contains data taken from Reference [25].

The fuel rod length was significantly shorter than full-length commercial rods to fit within the short length of the Halden reactor core. Slight differences in the pellet diameters, as defined in Table A.1, resulted in a variation in the initial radial fuel-clad gaps of 115 μm (Rod 1), 190 μm (Rod 2), and 25.5 μm (Rod 3).

A.2.1. Operating Conditions and Irradiation History

The reactor was operated with a coolant pressure of 3.4 MPa and an inlet temperature of 510 K. The power history was provided by experimentalists from Halden [26].

Table A.1.: IFA-431 Test Rod Specifications

Fuel Rod		
Overall length	m	0.635
Fuel stack height	m	0.5791
Nominal plenum height	mm	25.4
Number of pellets per rod		
Rod 1	mm	45
Rod 2	mm	44
Rod 3	mm	44
Fill gas composition		He
Fill gas pressure	MPa	0.1
Fuel		
Material		UO ₂
Enrichment	%	10
Density	%	95
Inner diameter	mm	1.752
Outer diameter		
Rod 1	mm	10.681
Rod 2	mm	10.528
Rod 3	mm	10.858
Pellet geometry		flat end
Grain diameter	μm	22-77
Cladding		
Material		Zr-2
Outer diameter	mm	12.789
Inner diameter	mm	10.909
Wall thickness	mm	0.94

A.3. Model Description

A.3.1. Geometry and Mesh

All three fuel rods were meshed using 2-D axisymmetric quadratic elements. For simplicity, the pellet stack was modeled as a single continuous fuel column. The thermocouple holes were modeled as closely to the experiment as possible at the top and bottom of the fuel rod. Figure A.1 shows a scaled view of the mesh for rod 1. Rods 2 and 3 were identical with exceptions to the thermocouple hole length and the pellet-clad gap width.

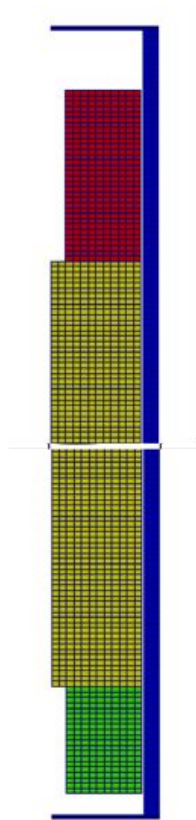


Figure A.1.: Scaled view of the finite element mesh for rod 1 (aspect ratio scaled 10x).

A.3.2. Material and Behavioral Models

The following material and behavioral models were used for the UO_2 fuel:

- ThermalFuel - NFIR: temperature and burnup dependent thermal properties
- VSwellingUO2: free expansion strains (swelling and densification)
- RelocationUO2: relocation strains, relocation activation threshold power set to 5 kW/m.
- Sifgr: Simplified fission gas release model

For the clad material, a constant thermal conductivity of 16 W/m-K was used and both thermal and irradiation creep were considered. The fast neutron flux used in the irradiation creep model was 1.6×10^{12} n/m²-s per W/m [5]. This value was multiplied by the power history (W/m) and the axial peaking factors to approximate the fast neutron flux.

A.3.3. Boundary and Operating Conditions

The clad outer wall temperature was assumed constant at 513.3 K. The input BOL power histories for Rods 1, 2, and 3 are shown in Figure A.2.

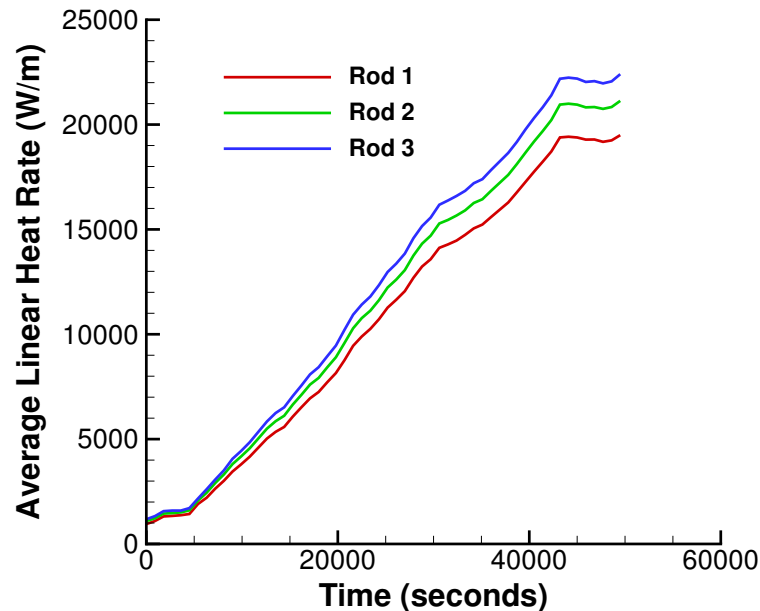


Figure A.2.: Input BOL power history for rods 1, 2, and 3.

A.3.4. Input files

The BISON input and all supporting files (power histories, axial power profile) are provided with the code distribution at bison/assessment/IFA_431/analysis.

A.3.5. Execution Summary

Table A.2.: Execution summary.

Rod	Machine	Operating System	Code Version
1	Mac Workstation	OS X	BISON 1.0
2	Mac Workstation	OS X	BISON 1.0
3	Mac Workstation	OS X	BISON 1.0

A.4. Results Comparison

BISON postprocessors were used to record the power and temperature histories at nodes corresponding to the upper and lower thermocouple positions.

A.4.1. Centerline Temperature at Beginning of Life

Initial comparisons were made to centerline fuel temperature measurements during the first rise to power, or the period referred to as the Beginning of Life (BOL). Comparisons during this period are important since they isolate several important aspects of fuel rod behavior before complexities associated with

higher burnups are encountered. For example, good prediction of BOL centerline temperature requires accurate models for the unirradiated fuel thermal conductivity, gap gas conductivity, thermal expansion of both the fuel and clad materials (which set the gap width), clad conductivity, and fuel relocation.

Figures A.3, A.4, and A.5 show centerline temperature comparisons at BOL for Rods 1, 2, and 3, respectively. Comparisons are excellent.

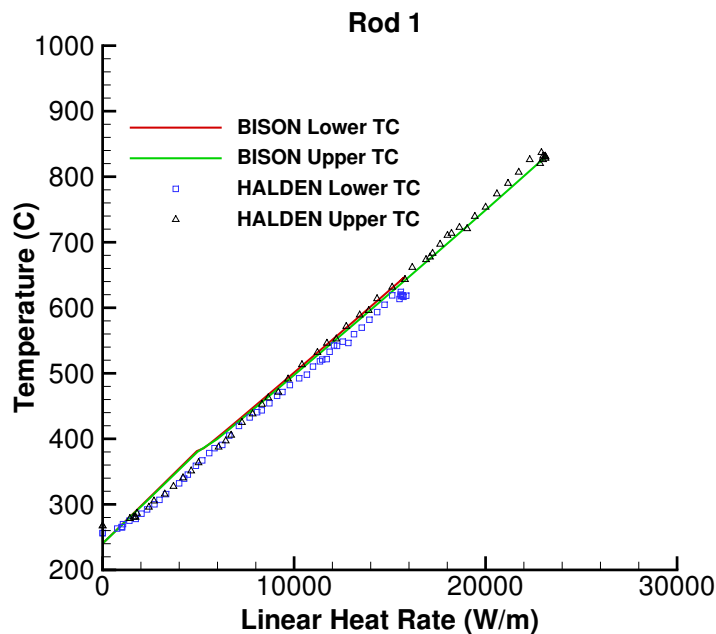


Figure A.3.: Comparison of measured and BISON predicted centerline temperatures at BOL for Rod 1.

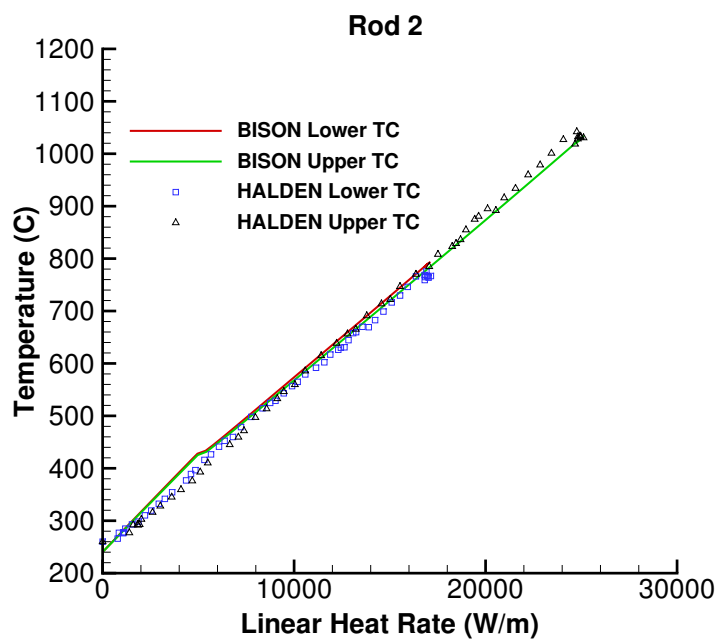


Figure A.4.: Comparison of measured and BISON predicted centerline temperatures at BOL for Rod 2.

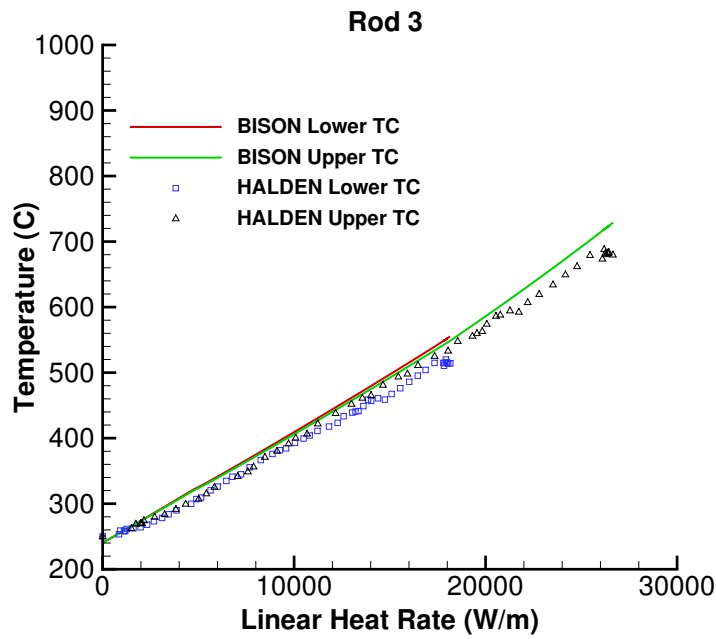


Figure A.5.: Comparison of measured and BISON predicted centerline temperatures at BOL for Rod 3.

A.5. Discussion

The recommended activation energy for the ESCORE relocation model implemented in BISON is 19.7 kW/m [11]. Based on experimental evidence of fuel cracking as a function of rod power, Wolfgang Wiesenack from Halden recommended lowering this activation threshold power to 5 kW/m. This lower value was further confirmed through a recent relocation calibration study [27] and is now used as the default value in BISON.

B. IFA 432 Rods 1, 2, and 3

B.1. Overview

The IFA-432 experiment was part of an effort by the US NRC to obtain well-characterized experimental data under conditions that simulate long-term steady LWR operation [24]. IFA-432 was a heavily instrumented fuel assembly irradiated in the Halden boiling water reactor from 1975 to 1984. The test rods initially contained fresh fuel and were operated at power levels near the upper bound for full-length commercial fuel rods.

The IFA-432 assembly included six instrumented rods, each with centerline temperature instrumentation in both the top and bottom ends of the fuel column. Three of the six rods (Rods 1, 2, 3) are the focus of this assessment. Rod 1 achieved a burnup of approximately 30 MWd/KgU, while rods 2 and 3 achieved burnups of approximately 45 MWd/kgU. Two of the temperature measurements failed prematurely. Rod 2 contained an ultrasonic thermometer at the top of the rod, which failed very early and no data were collected. The Rod 1 upper thermocouple failed after 150 days.

The IFA-432 assembly also contained neutron detectors, coolant thermocouples, a coolant flow meter, and a transducer to measure internal rod pressure.

B.2. Test Description

The three test rods considered here were designed to simulate BWR-6 rod cladding material and dimensions, and included only differences in fuel-cladding gap size. The general rod specifications are summarized in Table B.1 which contains data taken from Reference [25].

The fuel rod length was significantly shorter than full-length commercial rods to fit within the short length of the Halden reactor core. Slight differences in the pellet diameters, as defined in Table B.1, resulted in a variation in the initial radial fuel-clad gaps of 115 μm (Rod 1), 190 μm (Rod 2), and 38 μm (Rod 3).

B.2.1. Operating Conditions and Irradiation History

The reactor was operated with a coolant pressure of 3.4 MPa and an inlet temperature of 510 K. The power history was provided by experimentalists from Halden [28].

Table B.1.: IFA-432 Test Rod Specifications

Fuel Rod		
Overall length	m	0.635
Fuel stack height	m	0.5791
Nominal plenum height	mm	25.4
Number of pellets per rod		
Rod 1	mm	45
Rod 2	mm	44
Rod 3	mm	44
Fill gas composition		He
Fill gas pressure	MPa	0.1
Fuel		
Material		UO ₂
Enrichment	%	10
Density	%	95
Inner diameter	mm	1.752
Outer diameter		
Rod 1	mm	10.681
Rod 2	mm	10.528
Rod 3	mm	10.833
Pellet geometry		flat end
Grain diameter	μm	22-77
Cladding		
Material		Zr-2
Outer diameter	mm	12.789
Inner diameter	mm	10.909
Wall thickness	mm	0.94

B.3. Model Description

B.3.1. Geometry and Mesh

All three fuel rods were meshed using 2-D axisymmetric quadratic elements. For simplicity, the pellet stack was modeled as a single continuous fuel column. The thermocouple holes were modeled as closely to the experiment as possible at the top and bottom of the fuel rod. Figure B.1 shows a scaled view of the mesh for rod 1. Rods 2 and 3 were identical with exceptions to the thermocouple hole length and the gap width.

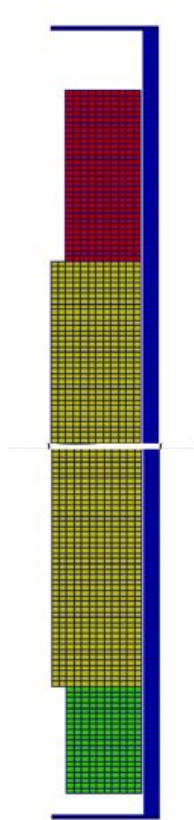


Figure B.1.: Scaled view of the finite element mesh for rod 1 (aspect ratio scaled 10x).

B.3.2. Material and Behavioral Models

The following material and behavioral models were used for the UO_2 fuel:

- ThermalFuel - NFIR: temperature and burnup dependent thermal properties
- VSwellingUO2: free expansion strains (swelling and densification)
- RelocationUO2: relocation strains, relocation activation threshold power set to 5 kW/m.
- Sifgr: Simplified fission gas release model

For the clad material, a constant thermal conductivity of 16 W/m-K was used and both thermal and irradiation creep were considered. The fast neutron flux used in the irradiation creep model was 1.6×10^{12} n/m²-s per W/m [5]. This value was multiplied by the power history (W/m) and the axial peaking factors to approximate the fast neutron flux.

B.3.3. Boundary and Operating Conditions

The clad outer wall temperature was assumed constant at 513.3 K. The input BOL power histories for Rods 1 and 3 are shown in Figure B.2.

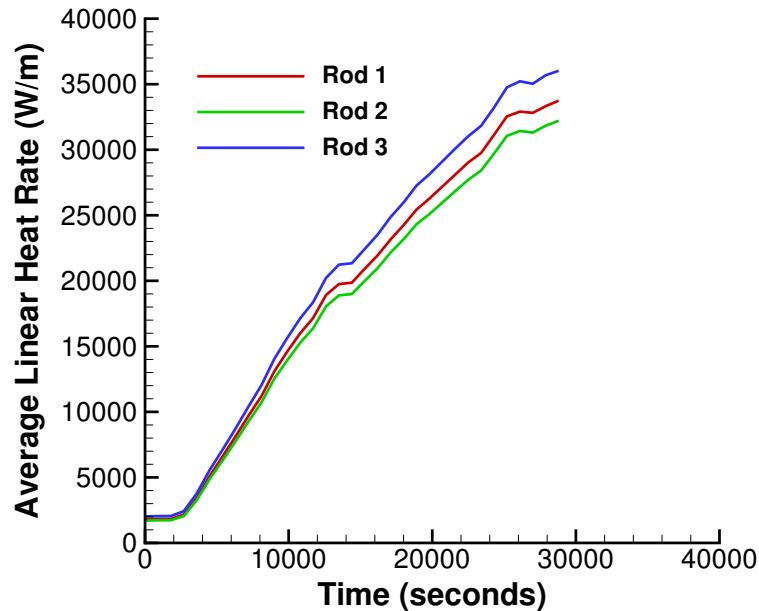


Figure B.2.: Input BOL power history for rods 1, 2, and 3

B.3.4. Input files

The BISON input and all supporting files (power histories, axial power profile) are provided with the code distribution at `bison/assessment/IFA_432/analysis`.

B.3.5. Execution Summary

Table B.2.: Execution summary.

Rod	Machine	Operating System	Code Version
1	Mac Workstation	OS X	BISON 1.0
2	Mac Workstation	OS X	BISON 1.0
3	Mac Workstation	OS X	BISON 1.0

B.4. Results Comparison

BISON postprocessors were used to record the power and temperature histories at nodes corresponding to the upper and lower thermocouple positions.

B.4.1. Centerline Temperature at Beginning of Life

Initial comparisons were made to centerline fuel temperature measurements during the first rise to power, or the period referred to as the Beginning of Life (BOL). Comparisons during this period are important since they isolate several important aspects of fuel rod behavior before complexities associated with

higher burnups are encountered. For example, good prediction of BOL centerline temperature requires accurate models for the unirradiated fuel thermal conductivity, gap gas conductivity, thermal expansion of both the fuel and clad materials (which set the gap width), clad conductivity, and fuel relocation.

Figures B.3, B.4, and B.5 show centerline temperature comparisons at BOL for Rods 1, 2, and 3, respectively. Note that for Rod 2, only lower thermocouple comparisons are possible since a gamma thermometer that failed to operate occupied this position in the rod [25]. Comparisons for all three rods are very good.

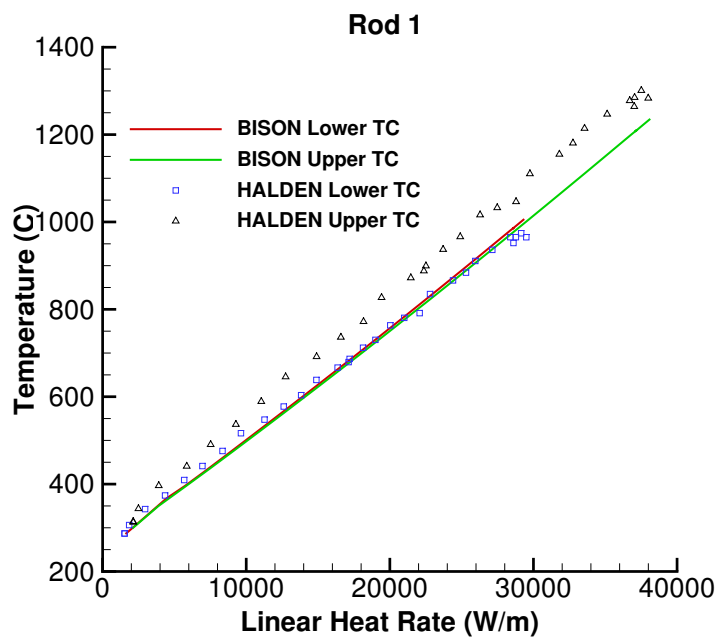


Figure B.3.: Comparison of measured and BISON predicted centerline temperatures at BOL for Rod 1.

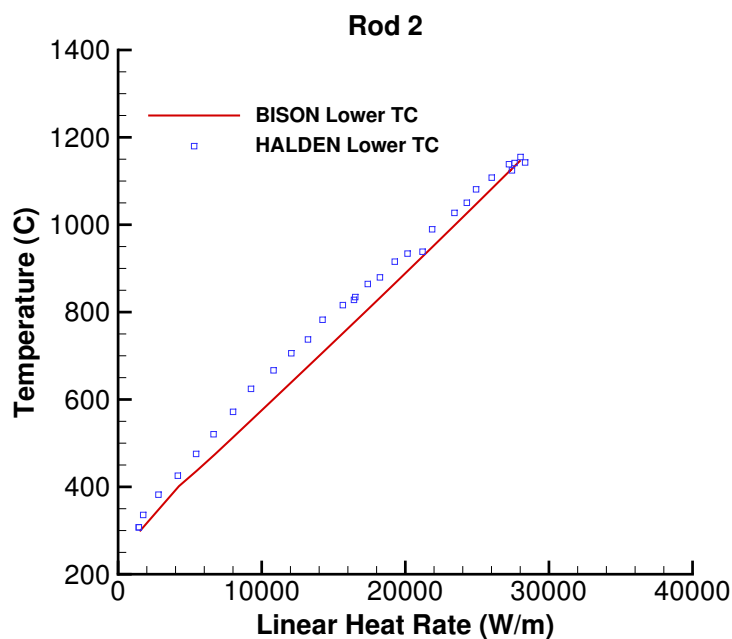


Figure B.4.: Comparison of measured and BISON predicted centerline temperatures at BOL for Rod 2.

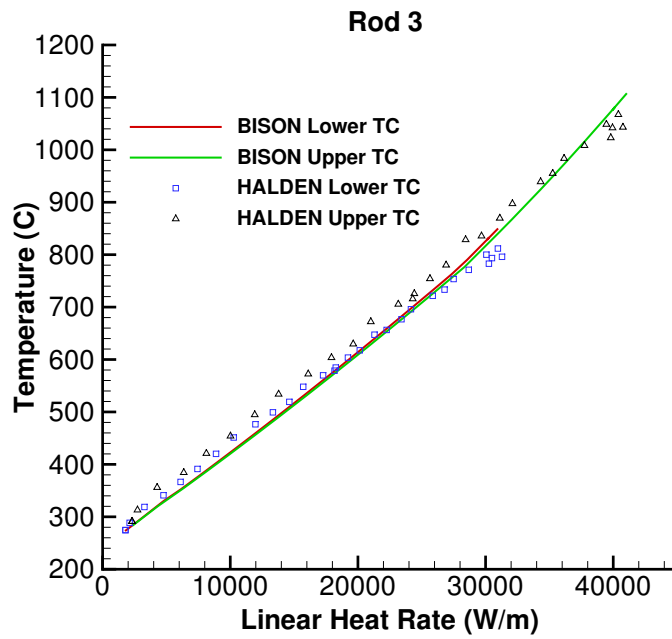


Figure B.5.: Comparison of measured and BISON predicted centerline temperatures at BOL for Rod 3.

B.5. Discussion

The recommended activation energy for the ESCORE relocation model implemented in BISON is 19.7 kW/m [11]. Based on experimental evidence of fuel cracking as a function of rod power, Wolfgang Wiesenack from Halden recommended lowering this activation threshold power to 5 kW/m. This lower value was further confirmed through a recent relocation calibration study [27] and is now used as the default value in BISON.

C. IFA 515.10 Rod A1

C.1. Overview

The IFA-515.10 Rod A1 experiment was irradiated in the Halden Boiling Water Reactor (HBWR) for approximately 6 years to a discharge burnup of ~ 86 MWd/kgU. Rod A1 was fitted with a fuel centerline expansion thermometer (ET) to measure the fuel centerline temperature during irradiation [29].

C.2. Test Description

C.2.1. Rod Design Specifications

Rod A1 in the IFA-515.10 series was an annular short rod (0.2455 m overall length) enriched to 11.8 %. The fuel and clad specifications are tabulated in Table C.1.

Table C.1.: IFA-515.10 rod A1 Test Rod Specifications

Fuel Rod		
Overall length	m	0.2455
Fuel stack height	m	0.212
Nominal plenum height	mm	19.0
Fill gas composition		He
Fill gas pressure	MPa	1.0
Fuel		
Material		UO ₂
Enrichment	%	11.8
Density	%	96.8
Inner diameter	mm	1.80
Outer diameter	mm	5.56
Pellet geometry		flat end
Grain diameter	μm	15.3
Insulator Pellet		
Material		Al ₂ O ₃
Inner diameter	mm	1.80
Outer diameter	mm	5.56
Pellet length	mm	5.0
Cladding		
Material		Zr-2
Outer diameter	mm	6.53
Inner diameter	mm	5.61
Zr-Barrier thickness	mm	0.05
Wall thickness	mm	0.46

C.2.2. Operating Conditions and Irradiation History

The HBWR operating conditions are tabulated in Table C.2. The reactor power history is shown in Figure C.1. The measured reactor coolant temperature was used as the boundary temperature on the clad outer surface.

Table C.2.: Operational input parameters.

Coolant temperature	C	227
Coolant pressure	MPa	3.4
Fast neutron flux	n/(cm ² ·s) per (kW/m)	1.6·10 ¹¹

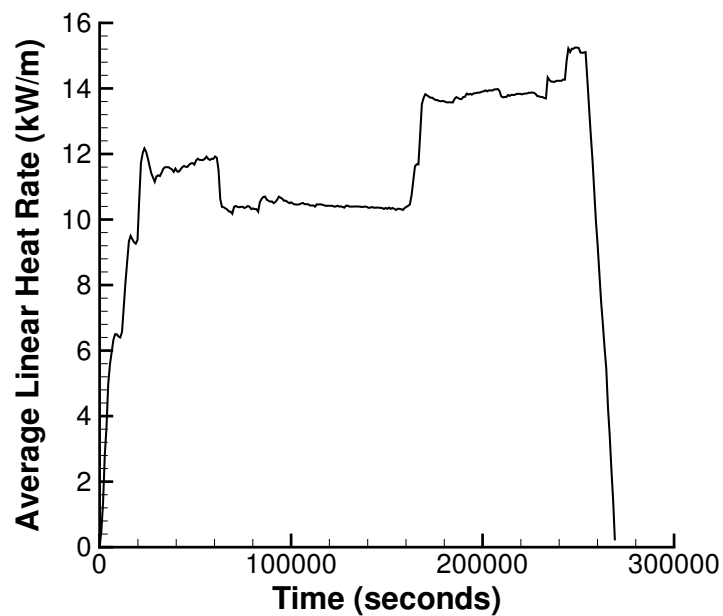


Figure C.1.: Halden irradiation BOL power profile for IFA-515.10 rod A1.

C.3. Model Description

C.3.1. Geometry and Mesh

The assumed geometry and mesh are shown in Figure C.2. The fuel pellet stack was modeled as a smeared column and the insulator pellets were neglected. The expansion thermometer was simulated as a metallic material bonded to the fuel, but given a very small elastic modulus so as not to influence the mechanical behavior of the fuel. The primary reason for including the expansion thermometer was to fill the fuel annulus in order to compute an accurate gas volume.

A 2-dimensional axisymmetric quadratic mesh was used. The fuel column was meshed with 210 axial and 13 radial elements and the expansion thermometer with 210 axial and 3 radial elements. The clad was meshed with 210 axial and 4 radial elements.



Figure C.2.: 2-D axisymmetric quadratic mesh for IFA-515.10 Rod A1 simulation. Note the figure is scaled radially by a factor of 5.

C.3.2. Material and Behavioral Models

The following material and behavioral models were used for the UO₂ fuel:

- ThermalFuel - NFIR: temperature and burnup dependent thermal properties
- VSwellingUO2: free expansion strains (swelling and densification)
- RelocationUO2: relocation strains, relocation activation threshold power set to 5 kW/m.
- Sifgrs: fission gas generation and release

For the clad material, a constant thermal conductivity of 16 W/m-K was used and both thermal and irradiation creep were considered.

C.3.3. Input files

The BISON input and all supporting files (power histories, axial power profile, clad surface temperature boundary condition, fast neutron flux history, etc.) for this case are provided with the code distribution at bison/assessment/IFA_515_RodA1/analysis.

C.3.4. Execution Summary

Table C.3.: Execution summary.

Machine	Operating System	Code Version
Mac Workstation	OS X	BISON 1.0

C.4. Results Comparison

A BISON postprocessor was used to extract the centerline temperature at a node near the axial mid-plane of the annular fuel. This provides an accurate representation of the average fuel centerline temperature since, in this case, the insulator pellets were ignored and there is no axial variation in fuel temperature.

C.4.1. Temperature

Initial comparisons were made to centerline fuel temperature measurements during the first rise to power, or the period referred to as the Beginning of Life (BOL). Comparisons during this period are important since they isolate several important aspects of fuel rod behavior before complexities associated with higher burnups are encountered. For example, good prediction of BOL centerline temperature requires accurate models for the unirradiated fuel thermal conductivity, gap gas conductivity, thermal expansion of both the fuel and clad materials (which set the gap width), clad conductivity, and fuel relocation.

Figure C.3 shows the fuel centerline temperature comparison as a function of average linear heat rate. The computed temperature was taken at a single point near the axial mid-plane of the annular fuel. BISON tends to under predict the measured temperature by roughly 30C during BOL. Considering uncertainty in the measured power and temperature, these comparisons are very good.

C.5. Discussion

In future studies, the insulator pellets will be included to more accurately represent axial temperature gradients in the fuel. Additionally, thermal and frictionless mechanical contact will be specified between the expansion thermometer and the fuel. This will permit direct comparison between the measured and computed axial displacement of the thermometer.

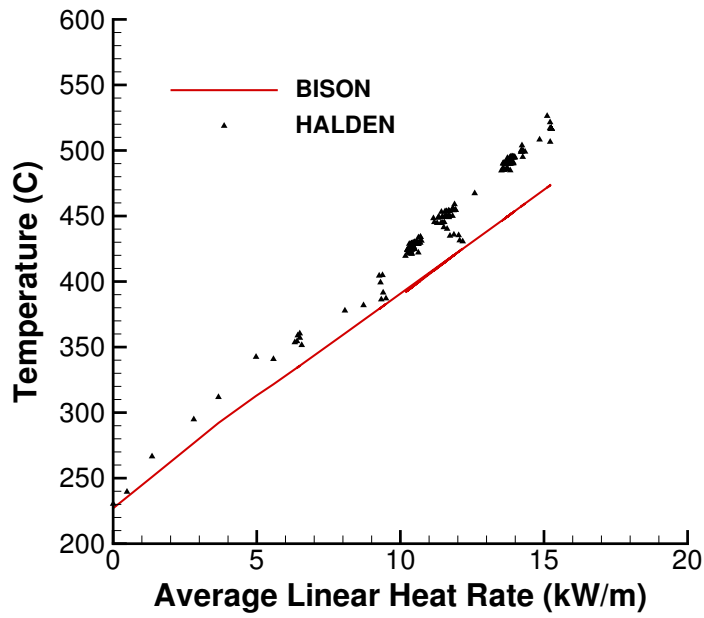


Figure C.3.: Comparison of measured and BISON predicted average fuel centerline temperature as a function of power at BOL.

D. IFA 597.3 Rods 7 and 8

D.1. Overview

The IFA-597.3 rod 8 experiment conducted at Halden utilized a re-fabricated rod from the Ringhals boiling water reactor (BWR) [19]. The mother rod was irradiated at a low average power of around 16 kW/m for approximately 12 years. The mother rod was then re-fabricated to a shorter length and fitted with a fuel centerline thermocouple and an internal pressure sensor [30], [31].

The IFA-597.3 rod 7 experiment is nearly identical to the IFA-597.3 rod 8 experiment with the exception that it was instrumented with an elongation detector as well. The two experiments saw nearly identical powers (differed by approximately 2 kW/m). Since these two experiments are essentially the same, they were modeled with one simulation for the comparisons.

D.2. Test Description

D.2.1. Rod Design Specifications

As stated in the previous section, both rods were nearly identical and comparisons for both experiments were modeled with one simulation. The specifications for rod 8 were used for the simulation. Rod 8 was a re-fabricated rod extracted from a full length rod. The hole for the thermocouple was at the top of the fuel stack and did not penetrate the entire fuel stack. The re-fabricated rod geometry is tabulated in Table D.1.

Table D.1.: IFA-597.3 Rod 8 Test Rod Specifications

Fuel Rod		
Overall length	m	0.3539
Fuel stack height	m	0.4098
Nominal plenum height	mm	0.0513
Mother Rod		
Fill gas composition		He
Fill gas pressure	MPa	0.1
Re-Fabricated Rod		
Fill gas composition		He
Fill gas pressure	MPa	0.5
Fuel		
Material		UO ₂
Enrichment	%	3.347
Density	%	95.5
Inner diameter	mm	2.5
Outer diameter	mm	10.439
TC hole length	mm	34.0
Pellet geometry		dishing one end
Grain diameter	μm	7.83
Pellet Dishing		
Dish diameter	cm	0.5
Dish depth	cm	0.01
Chamfer width	cm	0.07
Chamfer depth	cm	0.02
Cladding		
Material		Zr-2
Outer diameter	mm	12.25
Inner diameter	mm	10.65
Wall thickness	mm	0.8

D.2.2. Operating Conditions and Irradiation History

The power history for the base irradiation carried out at the Ringhals BWR is shown in Figure D.1. The experiment power history carried out at the Halden boiling water reactor (HBWR) is shown in Figure D.2. The measured clad surface temperature as a function of time is shown in Figure D.3. The other reactor operational parameters are tabulated in Table D.2.

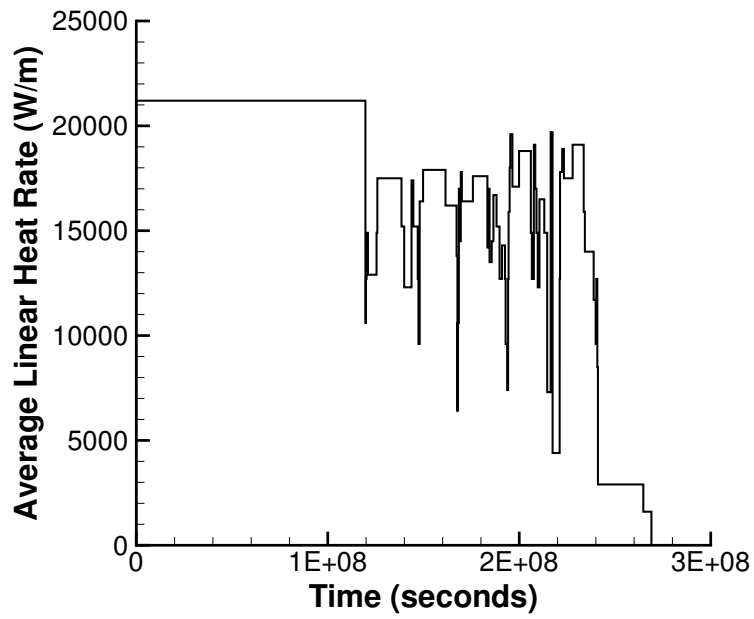


Figure D.1.: Base irradiation history for IFA-597.3, carried out at Ringhals BWR.

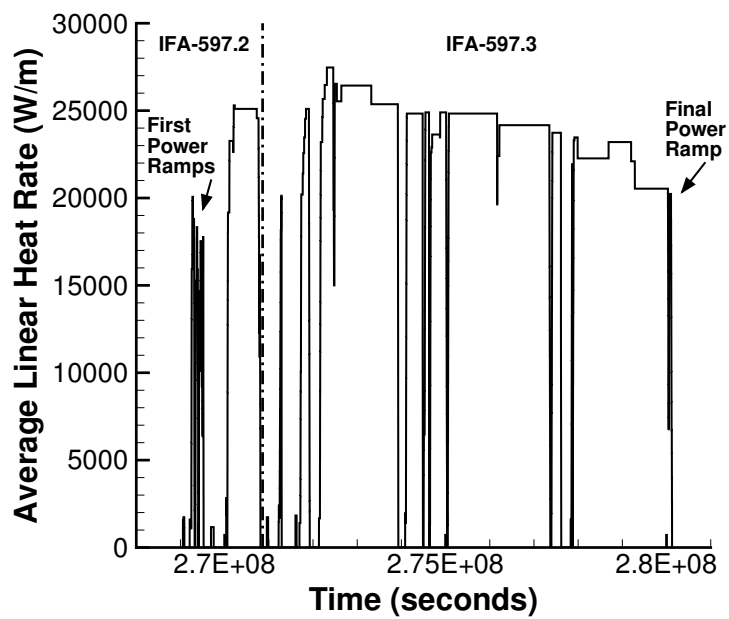


Figure D.2.: Halden irradiation periods for IFA-597.3 rod 8.

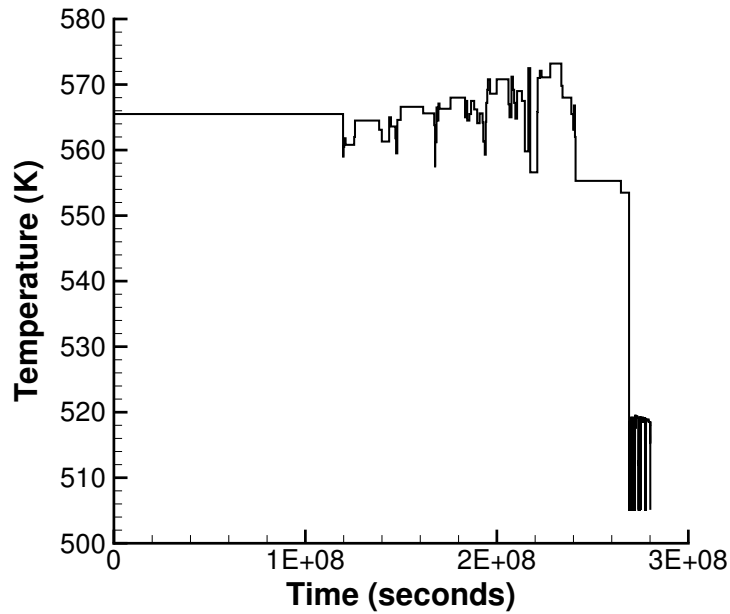


Figure D.3.: IFA-597.3 Rod8 clad surface temperature as a function of time.

Table D.2.: Operational input parameters.

Base Irradiation		
Coolant inlet temperature	C	286
Coolant pressure	MPa	7.0
Fast neutron flux	n/(cm ² ·s) per (kW/m)	2.3·10 ¹²
Power Ramps		
Coolant inlet temperature	C	232
Coolant pressure	MPa	3.2
Fast neutron flux	n/(cm ² ·s) per (kW/m)	1.6·10 ¹¹

D.3. Model Description

D.3.1. Geometry and Mesh

The re-fabricated rod geometry was modeled for the entire simulation. The rod was modeled with two smeared pellet blocks, one annular and one solid, to account for the thermocouple at the top of the fuel rod.

A 2D-RZ axisymmetric quadratic mesh was used to model the geometry of rod 8. The fuel mesh consisted of 128 axial nodes and 14 radial nodes (11 radial elements for the annular section) and the clad was meshed with 4 radial elements through the thickness. A section of the meshed fuel rod at the thermocouple location is shown in Figure D.4.

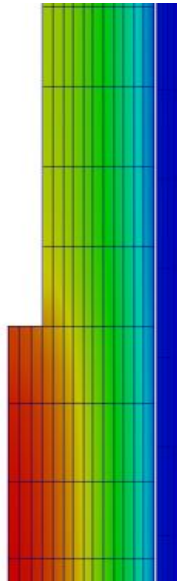


Figure D.4.: 2D-RZ axisymmetric mesh for IFA-597.3 Rod 8 simulation with temperature contour plot at thermocouple location.

D.3.2. Material and Behavioral Models

The following material and behavioral models were used for the UO₂ fuel:

- ThermalFuel - NFIR: temperature and burnup dependent thermal properties
- RelocationUO2: relocation strains
- Sifgrs: Simplified fission gas release model with a combined solid/gaseous swelling model based on fission gas release.

Material models for Zr-4 were used as a replacement for the Zr-2 clad. For the clad material, a constant thermal conductivity of 16 W/m-K was used and both thermal (primary and secondary) and irradiation creep were considered.

D.3.3. Input files

The BISON input and all supporting files (power histories, axial power profile, fast neutron flux history, etc.) for this case are provided with the code distribution at `bison/assessment/IFA_597_3/analysis`.

D.3.4. Execution Summary

Table D.3.: Execution summary.

Machine	Operating System	Code Version
Mac Workstation	OS X	BISON 1.0

D.4. Results Comparison

The IFA-597.3 Rod 8 experiment irradiated at Halden is used to demonstrate the code's capability to capture the fuel centerline temperature and the total fission gas released. The IFA-597.3 Rod 7 experiment is used to assess the code's capability to predict clad elongation during irradiation.

D.4.1. Temperature

Comparison of the measured and predicted fuel centerline temperature during the first four and final power ramps are shown in Figure D.5. Although BISON tends to under predict the temperature, considering uncertainties in the power and temperature measurements the comparisons are reasonable.

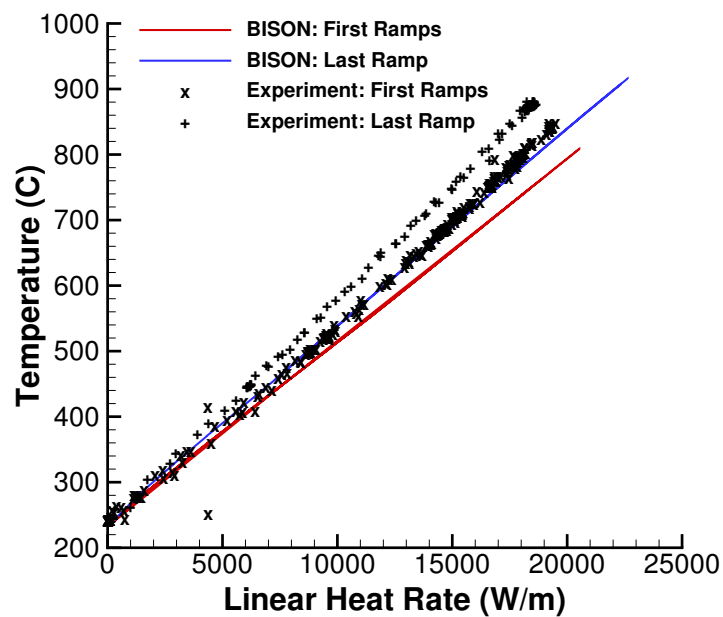


Figure D.5.: BISON fuel centerline temperature comparison to Halden experimental data.

D.4.2. Fission Gas Release

BISON under predicts the total FGR at the end of base irradiation and at the end of the power ramps. The pressure transducer that was used to measure the FGR reached its maximum operating limit at 68 MWd/kgU. The total fission gas release measured during the PIE puncture test was 15.8%. BISON predicts 1.8%. The BISON results compared to experimental data is shown in Figure D.6.

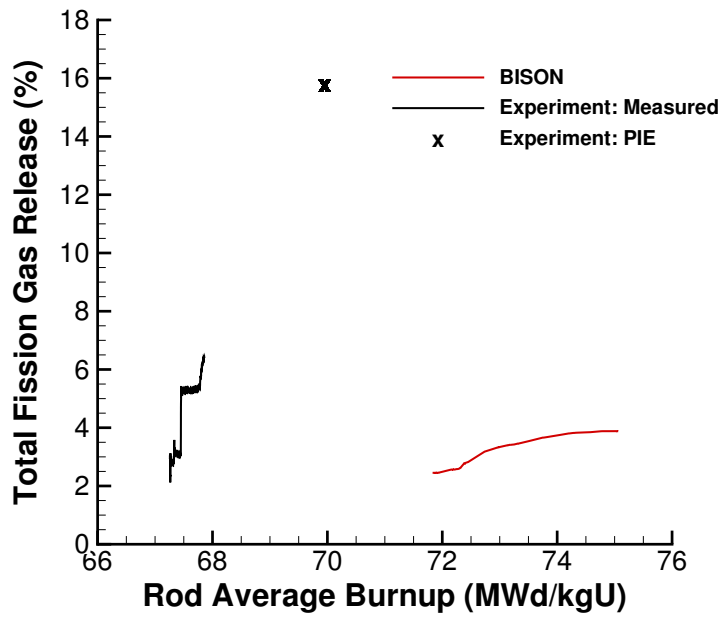


Figure D.6.: BISON fuel centerline temperature comparison to Halden experimental data.

D.4.3. Clad Elongation

The clad elongation was predicted with both frictionless contact between the fuel and clad and with glued contact between the fuel and clad, with the actual clad elongation lying between the two predictions.

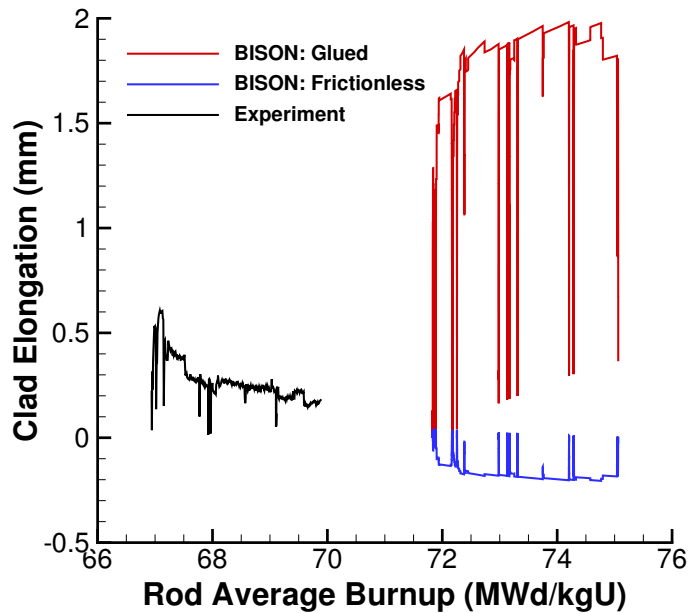


Figure D.7.: BISON fuel centerline temperature comparison to Halden experimental data.

D.5. Discussion

BISON over predicts the burnup which leads to a shift in the comparisons; this is currently being investigated.

It is recommended that this problem be revisited when frictional contact is ready for use in order to better predict the clad elongation during the power ramps.

E. Risø AN3

E.1. Overview

The Risø AN3 experiment conducted at the Risø DR3 water-cooled HP1 rig utilized a re-fabricated rod from the Biblis A pressurized water reactor (PWR) [19],[32]. The mother rod, CB8, was irradiated over four reactor cycles up to about 41 GWd/t, and re-fabricated to a shorter length. The re-fabricated rod, CB8-2R, was instrumented with a fuel centerline thermocouple and a pressure transducer. The fuel centerline temperature, fission gas release and rod internal pressure can be used for comparison.

E.2. Test Description

E.2.1. Rod Design Specifications

Rod CB8-2R was a re-fabricated rod extracted from a full length rod. The hole for the thermocouple was at the top of the fuel rod and did not penetrate the entire fuel stack. The re-fabricated rod geometry is tabulated in Table E.1.

Table E.1.: Risø AN3 Test Rod Specifications

Fuel Rod		
Overall length	m	0.39058
Fuel stack height	m	0.286
Nominal plenum height	mm	61.0
Mother Rod		
Fill gas composition		He
Fill gas pressure	MPa	2.31
Re-Fabricated Rod		
Fill gas composition		He
Fill gas pressure	MPa	1.57
Fuel		
Material		UO ₂
Enrichment	%	2.95
Density	%	93.74
Inner diameter	mm	2.5
Outer diameter	mm	9.053
Pellet geometry		both ends
Grain diameter	μm	6.0
Pellet Dishing		
Dish diameter	cm	0.665
Dish depth	cm	0.013
Chamfer width	cm	0.046
Chamfer depth	cm	0.016
Cladding		
Material		Zr-4
Outer diameter	mm	10.81
Inner diameter	mm	9.258
Wall thickness	mm	0.776

E.2.2. Operating Conditions and Irradiation History

The power history for the base irradiation carried out at the Biblis A PWR is shown in Figure E.1. The experiment power history carried out at the Risø DR3 facility is shown in Figure E.2. A prescribed axial profile for this experiment was provided in the FUMEX-II data [19]. The measured clad surface temperature as a function of time was also provided in the FUMEX-II data [19] and used as a boundary condition for this simulation. The other reactor operation parameters are tabulated in Table E.2.

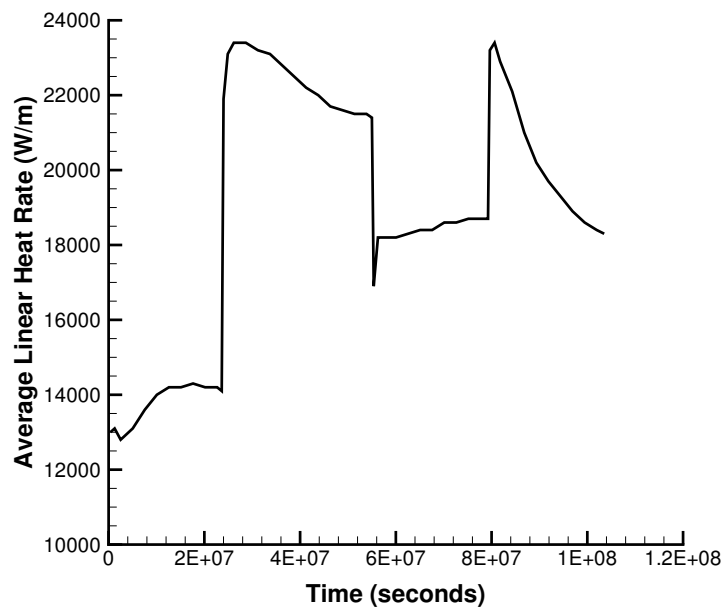


Figure E.1.: Base irradiation history for fuel segment CB8, carried out at Biblis A PWR.

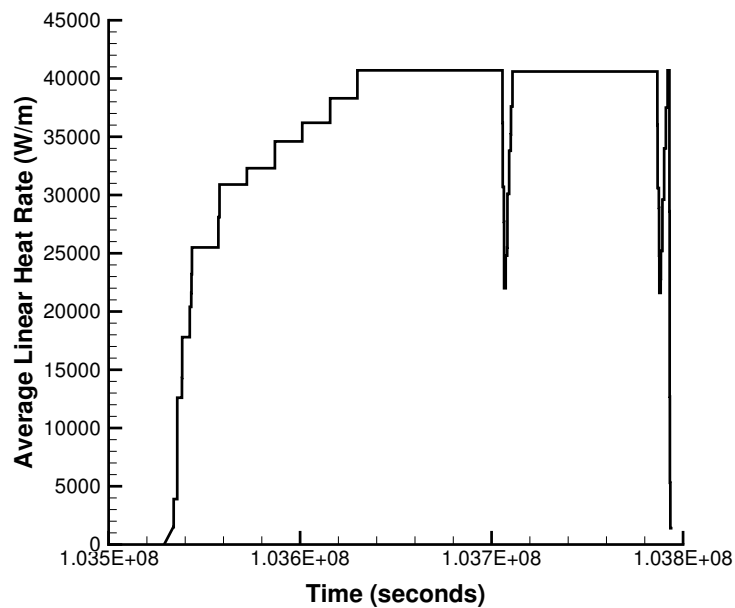


Figure E.2.: Risø DR3 irradiation period for test AN3 (CB8-2R).

Table E.2.: Operational input parameters.

Base Irradiation		
Coolant inlet temperature	C	287.7
Coolant pressure	MPa	15.52
Fast neutron flux	n/(cm ² ·s) per (kW/m)	3.4·10 ¹²
Power Ramps		
Coolant inlet temperature	C	NA
Coolant pressure	MPa	15.3
Fast neutron flux	n/(cm ² ·s) per (kW/m)	4.0·10 ¹¹

E.3. Model Description

E.3.1. Geometry and Mesh

The re-fabricated rod geometry was modeled for the entire simulation considering a smeared column of flat ended pellets, with the top pellets containing the hole for the thermocouple. The plenum height was adjusted such that the plenum volume at the beginning of the bump test was approximately 7.0 cm³. The entire fuel stack was shifted up from the bottom of the clad by 5.1 mm, which is the height of the insulator pellet at the bottom of the fuel rod.

A 2-dimensional axi-symmetric linear mesh was used to model the geometry of the rod used in the AN3 experiment. The fuel was meshed considering two fuel pellet types. The first pellet type was 4.1 cm in length with a hole down the center, the second pellet type was 24.5 cm in length with no hole down the center. The first pellet type's mesh consisted of 29 axial nodes and 10 radial nodes (for an aspect ratio of 4.07). The second pellet type's mesh consisted of 166 axial nodes and 13 radial nodes (for an aspect ratio of 3.93). The clad mesh consisted of 131 axial nodes and 3 radial nodes. Figure E.3 shows the top section of the mesh at the thermocouple location with a temperature contour plot.

E.3.2. Material and Behavioral Models

The following material and behavioral models were used for the UO₂ fuel:

- ThermalFuel - NFIR: temperature and burnup dependent thermal properties
- VSwellingUO2: free expansion strains (swelling and densification)
- RelocationUO2: relocation strains, relocation activation threshold power set to 5 kW/m.
- Sifgrs: fission gas release model

For the clad material, a constant thermal conductivity of 16 W/m-K was used and both thermal and irradiation creep were considered.

E.3.3. Boundary and Operating Conditions

The Risø DR3 irradiation period for the AN3 test shown in Figure E.2 was appended to the base irradiation power history shown in Figure E.1. It was assumed that the clad temperature during the down time between base irradiation and the Risø test was 500K. The fast neutron flux was input as a function of power and scaled to 4.9e17.

E.3.4. Input files

The BISON input and all supporting files (power histories, axial power profile, fast neutron flux history, etc.) for this case are provided with the code distribution at bison/assessment/Riso_AN3/analysis.

E.3.5. Execution Summary

Table E.3.: Execution summary.

Machine	Operating System	Code Version
Mac Workstation	OS X	BISON 1.0

E.4. Results Comparison

The Risø AN3 experiment is used to assess the code's capability to capture the fuel centerline temperature and the integral fuel rod fission gas release. Fuel centerline temperature and fission gas release data from the TRANSURANUS and ENIGMA codes were digitized from the FUMEX-II report [5] for comparison with the BISON predictions.

E.4.1. Temperature

BISON predicts the fuel centerline temperature well (see Figure E.3) and is comparable with other well known fuel performance codes. The fuel centerline temperature is taken at a node approximately 36.4 mm from the top of the fuel stack (black dot on mesh in Figure E.3).

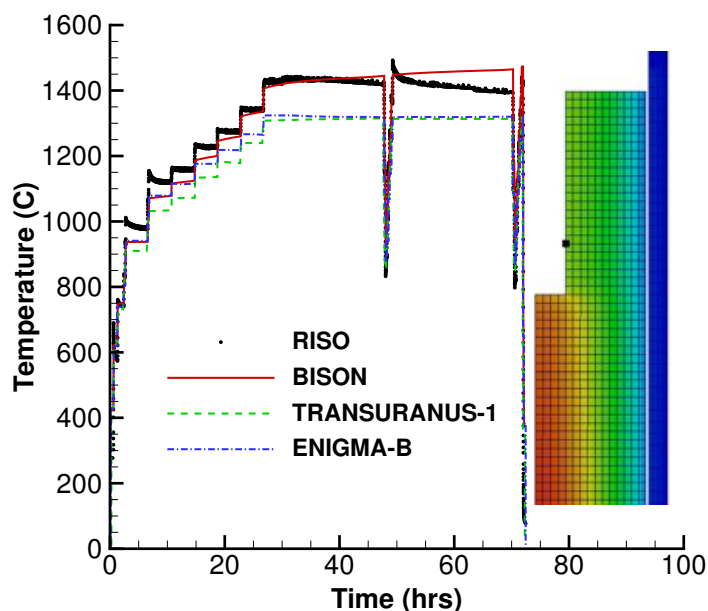


Figure E.3.: BISON fuel centerline temperature comparison to Risø experimental data and the fuel performance codes TRANSURANUS and ENIGMA with a temperature contour plot at thermocouple location.

E.4.2. Fission Gas Release

The calculated integral fuel rod fission gas release is compared to the measured data, as well as with the TRANSURANUS and ENIGMA predictions, in Figure E.4. In view of the uncertainties involved in FGR modeling, the predictive accuracy is satisfactory. When compared to other codes, BISON's prediction of total FGR is excellent, with many codes underpredicting the fission gas release at the end of life by more than a factor of 2 [5].

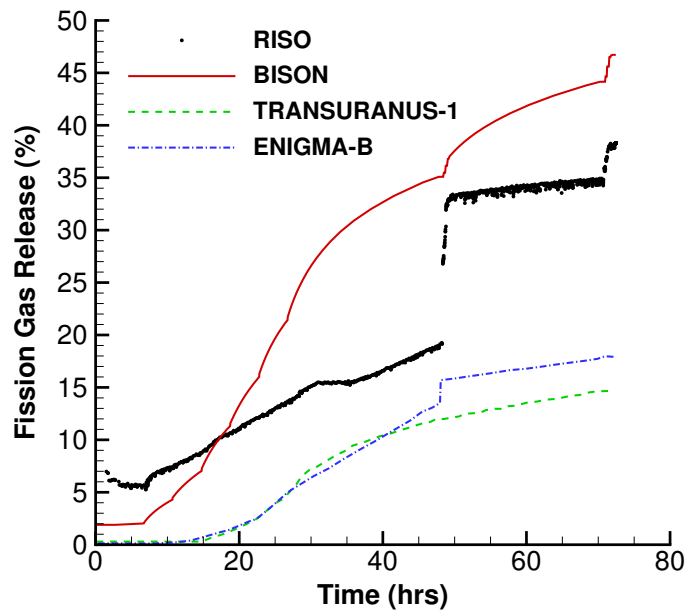


Figure E.4.: BISON total fission gas release comparison to Risø experimental data.

F. AREVA Idealized Case

F.1. Overview

The AREVA Idealized Case is an optimal case designed to simulate idealized commercial power plant operation. This case was based on measurements for three rods operated for 3, 4, and 7 cycles in a commercial French pressurized water reactor (PWR). The three rods chosen experienced similar power histories, allowing for three fission gas release measurements for a single power history. The maximum fuel rod burnup is approximately 81.5 MWd/kgU with a total fission gas release of approximately 9% [33].

F.2. Test Description

F.2.1. Rod Design Specifications

The rod simulated for this particular case was based on an idealized commercial reactor fuel rod. Details of the rod geometry and specifications are summarized in Table F.1.

Table F.1.: AREVA Idealized Case Test Rod Specifications

Fuel Rod		
Fuel stack length	m	3.65
Nominal plenum volume	cm ³	8.04
Number of pellets per rod		275
Fill gas composition		He
Fill gas pressure	MPa	1.6
Fuel		
Material		UO ₂
Enrichment	%	4.5
Density	%	95
Outer diameter	mm	8.085
Pellet geometry		dished
Grain diameter	μm	15.6
Pellet Dishing (if applicable)		
Dish diameter	mm	6.0
Dish depth	mm	0.31
Chamfer width	mm	0.5425
Chamfer depth	mm	0.27
Cladding		
Material		Zr-4 (stress-relieved)
Outer diameter	mm	9.5
Inner diameter	mm	8.25
Wall thickness	mm	0.625

F.2.2. Operating Conditions and Irradiation History

The operating conditions for this simulation were based on power cycles in a commercial French PWR. The operating conditions used are shown in Table F.2.

Table F.2.: Operational input parameters.

Coolant inlet temperature	C	282
Coolant pressure	MPa	15.5
Coolant mass flow rate	kg/m ² -sec	3700

F.3. Model Description

F.3.1. Geometry and Mesh

The fuel rod geometry specified in Table F.1 was used as a basis for the mesh used in this simulation. The fuel pellets were meshed as a single smeared fuel column. The mesh consists of 1375 axial elements and 12 radial elements in the fuel, and 1375 axial elements and 4 radial elements in the clad, see Figure F.1. This simulation was meshed as a 2D-RZ axisymmetric geometry with quadratic elements.

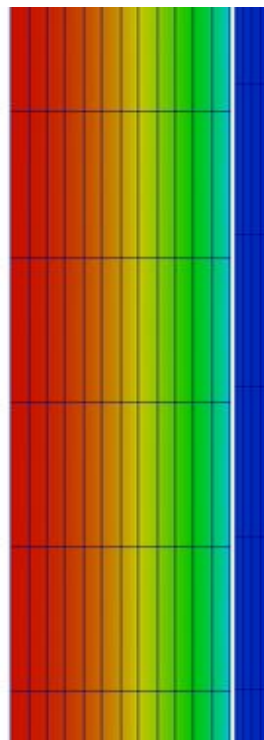


Figure F.1.: Section of BISON mesh with temperature contour.

F.3.2. Material and Behavioral Models

The following material and behavioral models were used for the UO₂ fuel:

- ThermalFuel - NFIR: temperature and burnup dependent thermal properties
- RelocationUO2: relocation strains, relocation activation threshold power set to 5 kW/m.
- Sifgrs: coupled fission gas release and swelling model

For the clad material, a constant thermal conductivity of 16 W/m-K was used and both thermal and irradiation creep were considered.

F.3.3. Boundary and Operating Conditions

The power history used for this simulation is shown in Figure F.2, with axial peaking factors shown in Figure F.3. The average fast neutron flux was input as a function as well and is shown in Figure F.4 with axial peaking factors shown in Figure F.5. The clad temperature was calculated using the coolant channel model.

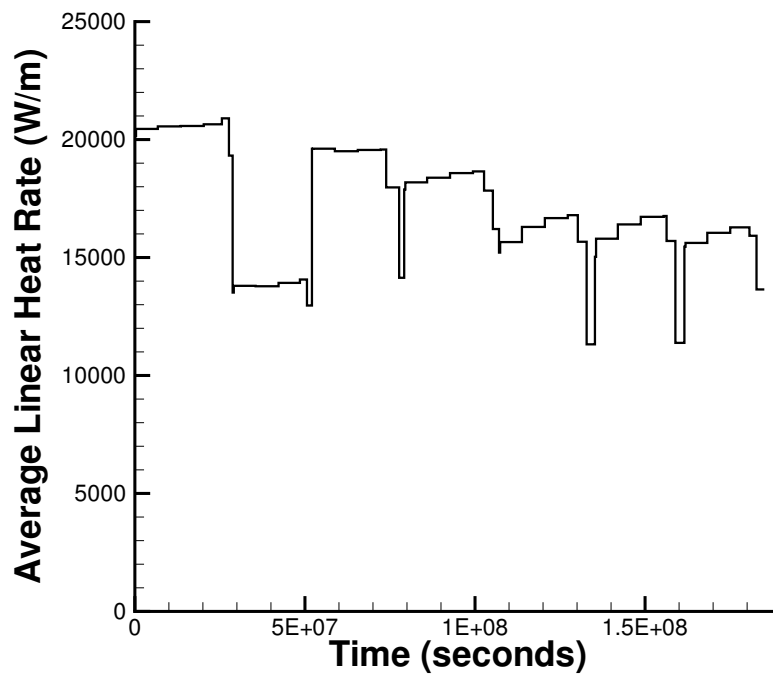


Figure F.2.: BISON input power history for the AREVA Idealized Case.

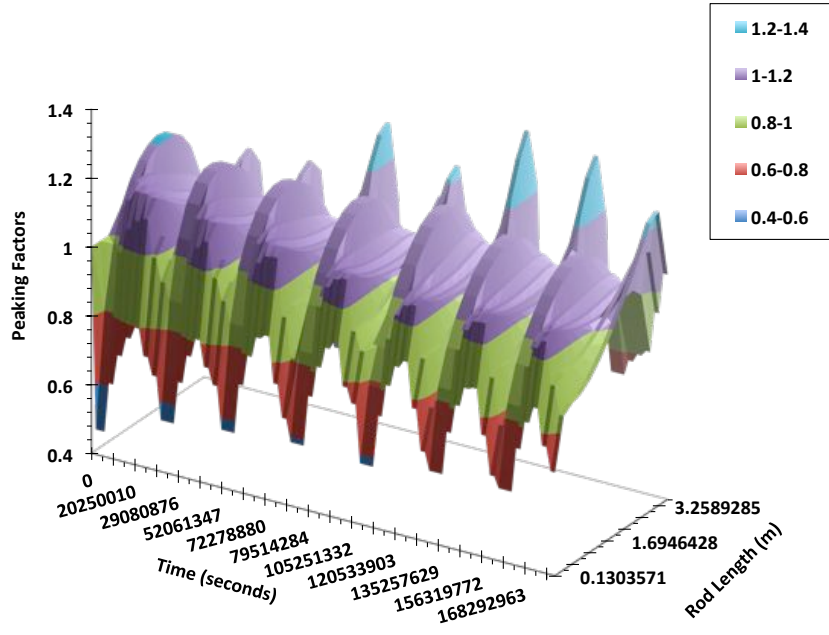


Figure F.3.: BISON input power axial peaking factors for the AREVA Idealized Case.

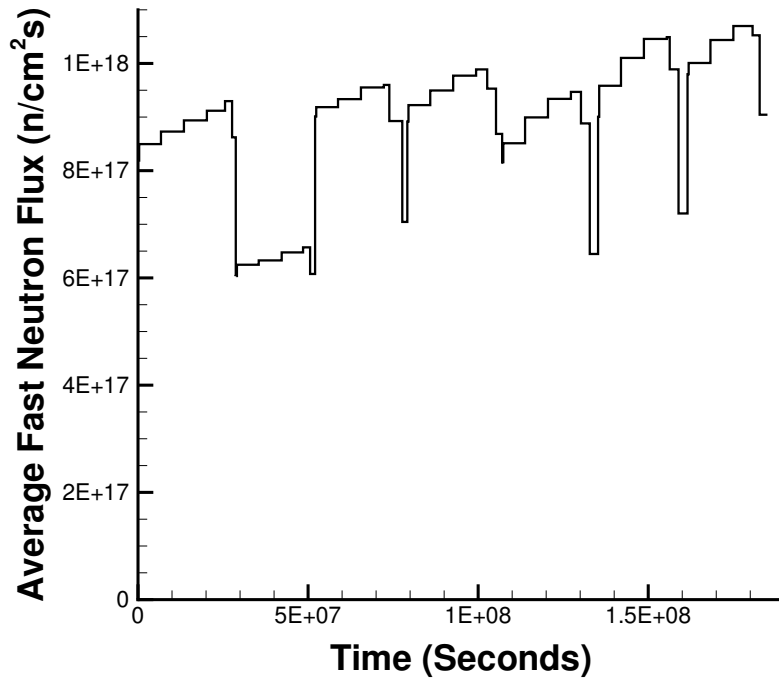


Figure F.4.: BISON input average fast neutron flux for the AREVA Idealized Case.

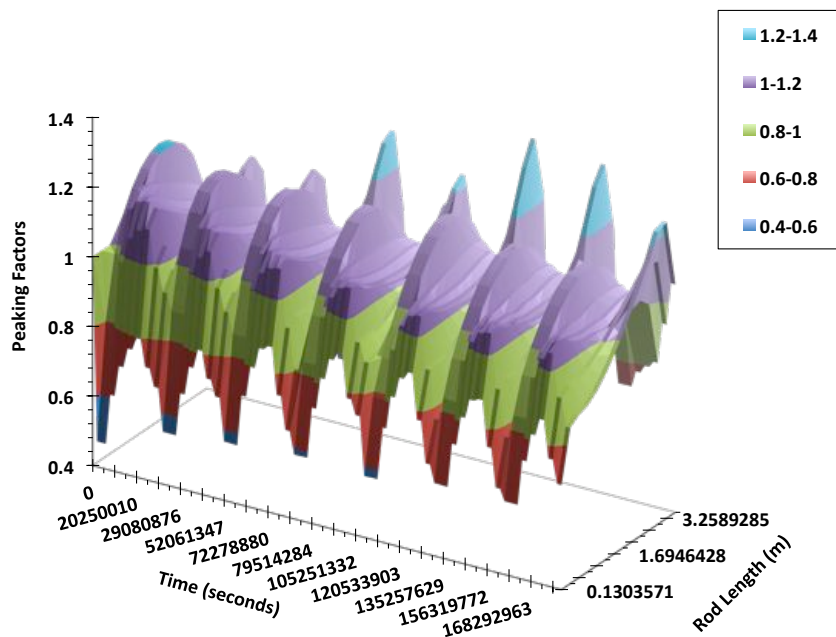


Figure F.5.: BISON input fast neutron flux axial peaking factors for the AREVA Idealized Case.

F.3.4. Input files

The BISON input and all supporting files (power histories, axial power profile, fast neutron flux history, etc.) for this case are provided with the code distribution at `bison/assessment/AREVA_idealized_case/analysis`.

F.3.5. Execution Summary

Table F.3.: Execution summary.

Machine	Operating System	Code Version
Mac Workstation	OS X	BISON 1.0

F.4. Results Comparison

F.4.1. Fission Gas Release

The expected fission gas release values are shown in Table F.4 [33].

Table F.4.: Expected FGR values.

End of cycle	Insertion time (d)	Burnup (MWd/kg(HM))	Expected FGR value (%)
3	916.4	36.6	0.5+0.5/-0.2
4	1239.1	49.7	1.9+1.0/-0.7
7	2141.9	81.5	9.0+2.5/-2.0

BISON predicts the total fission gas release reasonably well during the early and mid-burnup regimes, however FGR is under predicted at high burnup. BISON also compares well with other well known fuel performance codes, see Figure F.6.

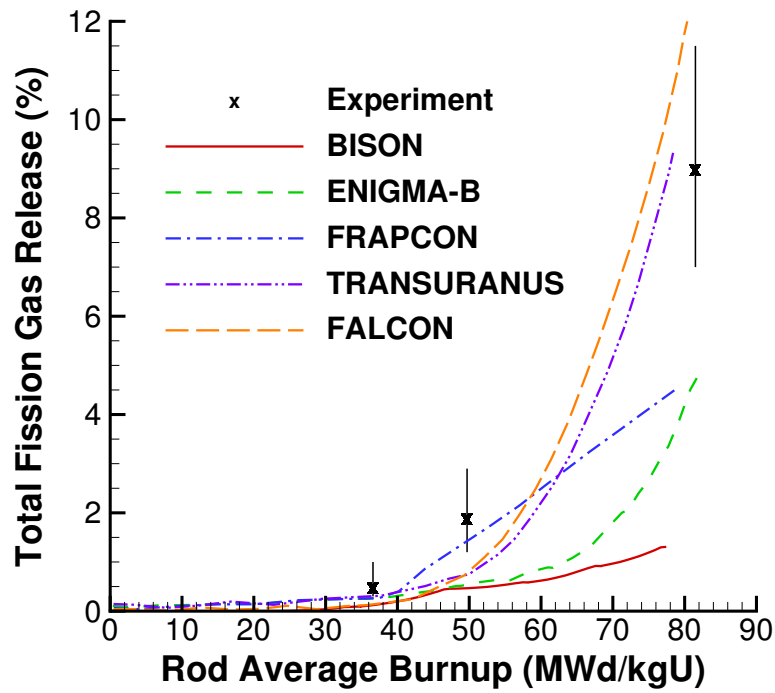


Figure F.6.: BISON predicted fission gas release in comparison to measured data and multiple fuel performance codes (code data digitized from FUMEX-III report [33]).

F.5. Discussion

Fuel creep was not modeled at this time. Fuel creep will be considered upon availability of some type of fuel cracking model.

G. FUMEX-II Simplified Cases

G.1. Overview

Over the last few decades, the International Atomic Energy Agency (IAEA) has supported several programs related to nuclear power reactor fuel behavior and fuel behavior modeling. These efforts have collected fuel behavior experimental data, fuel irradiation experiment and hardware descriptions, and fuel modeling code results to develop a useful database of information for code assessment and to determine the maturity of currently existing fuel performance codes. One such program was the Fuel Modeling at Extended Burnup (FUMEXII [19]) program. This program, conducted from 1999-2007, outlined relevant collections of analytical exercises and appropriate experiments and encouraged participants to submit calculation results for a wide variety of fuel performance experiments in a format that readily allowed comparisons between specific codes and to experiment data when available. Given the success of this approach and ready access to the results, we chose to use some test cases from the FUMEXII program for initial assessment of certain BISON code elements. In particular, FUMEXII participants devoted significant effort to fission gas release (FGR) and an impressive compilation of experiment data and code results is given in Ref. [19].

FGR is of particular interest for the present BISON assessment since calculation of fuel centerline temperature and radial and axial temperature distribution depends heavily on fission gas generation in the pellets, migration of the gas to grain boundaries, and eventual release to the fuel pin gap and plenum. FUMEXII Case No. 27, so-called 'Simplified cases', provide an ideal basis for examining the BISON FGR model(s) performance and comparison of BISON results with results from other fuel performance codes that participated in the FUMEXII exercises. The first of the simplified cases, 27(1) focused on the Vitanza criterion [34], which is the comparison of fuel centerline temperature versus burnup at onset of FGR (e.g. 1% release). The second case was to assess the codes' ability to predict total FGR as a function of burnup up to 100 MWd/kgU. Four separate simulations were used for this case:

- 27(2a) a constant power of 15 kW/m from BOL to 100 MWd/kgU,
- 27(2b) a linearly decreasing power from 20 kW/m at BOL to 10 kW/m at 100 MWd/kgU,
- 27(2c) more realistic power history supplied by G Rossiter of BNFL,
- 27(2d) idealized 'real' history supplied by F Sontheimer of FANP.

G.2. Test Description

G.2.1. Rod Design Specifications

For Case 27(1), 27(2a), and 27(2b), a standard fuel description representative of a boiling water reactor (BWR) fuel rod typically irradiated in the Halden reactor was specified. The rod plenum was specified as being large as to avoid thermal feedback, the rod plenum fill gas was helium at 0.5 MPa (5 bar). The fuel pellet was solid and flat ended (no chamfer, no dish) UO₂ with 13% ²³⁵U enrichment and a grain diameter of 15 microns. Cladding consisted of standard Zr-2. In the Halden reactor, fast neutron flux is typically assumed negligible and thus irradiation induced cladding creep is negligible. Also, the axial power profile in Halden is flat. The detailed specification of the pellet, cladding, and other information relevant to the exercise is shown in Table G.1.

Table G.1.: FUMEX-II 27(1), 27(2a), and 27(2b) Fuel Rod/Pellet Specifications.

Fuel Rod		
Fuel stack length	m	0.0127
Number of pellets per rod		1
Fill gas composition		He
Fill gas pressure	MPa	0.5
Fuel		
Material		UO ₂
Enrichment	%	13
Density	%	95
Outer diameter	mm	10.61
Pellet geometry		Flat Ended
Grain diameter	μm	15
Cladding		
Material		Zr-2
Outer diameter	mm	12.7
Inner diameter	mm	10.8
Wall thickness	mm	0.95

Table G.2.: FUMEX-II 27(2c) Fuel Rod/Pellet Specifications.

Fuel Rod		
Fuel stack length	m	3.658
Nominal plenum length	mm	162
Number of pellets per rod		275
Fill gas composition		He
Fill gas pressure	MPa	2.5
Fuel		
Material		UO ₂
Enrichment	%	8
Density	%	95
Outer diameter	mm	8.2
Pellet length	mm	9.8
Pellet geometry		dished
Grain diameter	μm	75
Pellet Dishing (no chamfers)		
Dish diameter	mm	5.24
Dish depth	mm	0.3
Cladding		
Material		Zr-4
Outer diameter	mm	9.5
Inner diameter	mm	8.36
Wall thickness	mm	0.57

For case 27(2c) and 27(2d) the fuel rod specifications were provided by BNFL (Table G.2) and FANP (Table G.3), respectively.

Table G.3.: FUMEX-II 27(2d) Fuel Rod/Pellet Specifications.

Fuel Rod		
Fuel stack length	m	3.5
Total free volume	cm ³	30
Number of pellets per rod		318
Fill gas composition		He
Fill gas pressure	MPa	2.2
Fuel		
Material		UO ₂
Enrichment	%	4
Density	%	95.5
Outer diameter	mm	9.12
Pellet length	mm	11.0
Pellet geometry		standard UO ₂
Grain diameter	μm	10
Cladding		
Material		Zr-4
Outer diameter	mm	10.75
Inner diameter	mm	9.29
Wall thickness	mm	0.73

G.2.2. Operating Conditions and Irradiation History

To match the Vitanza Threshold (described above) multiple simulations are ran at multiple powers until 1% FGR is reached. This was done for 20, 25, 30, 35, 40, and 45 kW/m. For case 27(2a) a constant power of 15 kW/m was used up to a burnup of 100 MWd/kgU. The power for case 27(2b) linearly decreased from 20 kW/m at BOL to 10 kW/m at a burnup of 100 MWd/kgU. Typical Halden BWR (HBWR) conditions were used for the operating conditions (fast neutron flux of $1.6E11$ n/cm²-sec per kW/m, coolant temperature of 232 C, and a coolant pressure of 3.2 MPa) for cases 27(1), 27(2a), and 27(2b).

The power history used for case 27(2c) is shown in Figure G.1(a), the power is provided as a thermal power in the fuel. The ratio of thermal heat to total heat for the rod is 0.975, thus the input power is scaled by a factor of 1.025641 as BISON requires the total fission power as input. The fast neutron flux was specified as a function and is shown in Figure G.1(b). The coolant pressure was specified as 15.5 MPa with an average clad temperature of 325 C.

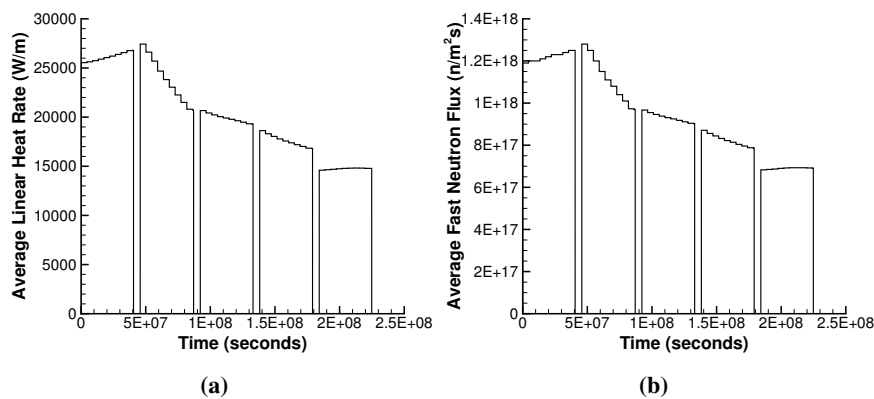


Figure G.1.: (a) Case 27(2c) average linear heat rate (b) Case 27(2c) average fast neutron flux.

The power history used for case 27(2d) is shown in Figure G.2. The fast neutron flux had a suggested value of $4E16$ n/m²-sec per kW/m. The coolant pressure was 15.5 MPa, with a coolant temperature of 290 C and a mass flow rate of 0.4 kg/s.

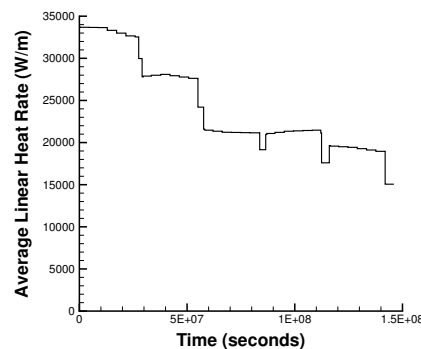


Figure G.2.: Case 27(2d) average linear heat rate.

G.3. Model Description

G.3.1. Geometry and Mesh

Case 27(1)

For this exercise, the main interest was interaction between the fission gas generation and release and the thermal behavior of the fuel. As such, several simplifications could be made. First, since fractional fission gas release was of prime interest, only a single fuel pellet reflecting the parameters given in Table G.1 was modeled. Second, since fuel-cladding interaction was not of interest, the cladding was removed and only the fuel pellet was modeled. A convective boundary condition representative of Halden operating conditions was applied directly to the pellet outer radius and the top and bottom of the pellet were insulated.

Figure G.3 shows the mesh used for BISON calculation of the Vitanza criteria. This mesh represents a 2D-RZ axi-symmetric geometry and with 12 radial and 8 axial quadratic elements.

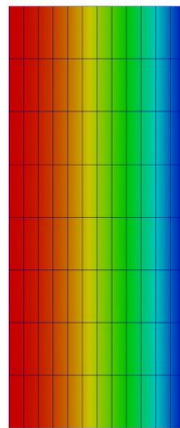


Figure G.3.: BISON single pellet mesh used for Vitanza Criteria calculation. Fuel temperature profile shown at 1% FGR for LHR of 45 kW/m.

Cases 27(2a) and 27(2b)

A similar mesh was used for cases 27(2a) and 27(2b), except the clad was modeled in these two cases. This mesh consisted of 12 radial and 8 axial quadratic elements in the fuel and 4 radial elements in the clad (see Figure G.4).

Case 27(2c)

Fuel rod specifications in Table G.2 were used to generate the mesh for case 27(2c). The fuel rod was meshed as a 2D-RZ axi-symmetric geometry, with 11 radial and 5 axial quadratic elements per fuel pellet. The clad thickness was meshed with 4 radial quadratic elements. A section of the fuel rod is shown in Figure G.5.

Case 27(2d)

Fuel rod specifications in Table G.3 were used to generate the mesh for case 27(2d). The fuel rod was meshed as a 2D-RZ axi-symmetric geometry, with 11 radial and 4 axial quadratic elements per fuel pellet. The clad thickness was meshed with 4 radial quadratic elements. A section of the fuel rod is shown in Figure G.6.

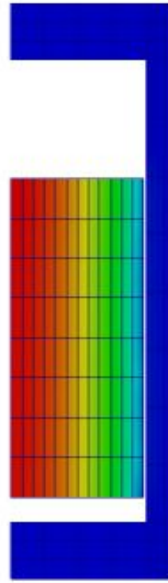


Figure G.4.: BISON mesh used for cases 27(2a) and 27(2b). Temperature contour of 27(2a) at a burnup of 100 MWd/kgU.

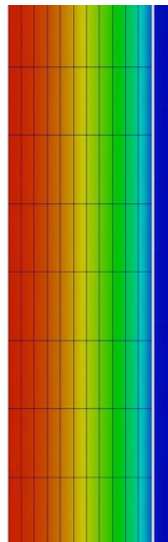


Figure G.5.: BISON mesh used for cases 27(2c). Temperature contour at a burnup of approximately 100 MWd/kgU.

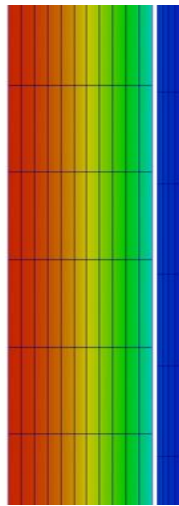


Figure G.6.: BISON mesh used for cases 27(2d). Temperature contour at a burnup of approximately 67.5 MWd/kgU.

G.3.2. Material and Behavioral Models

The following material and behavioral models were used for the UO₂ fuel:

- ThermalFuel - NFIR: temperature and burnup dependent thermal properties
- VSwellingUO2: provides free expansion strains (swelling and densification)
- CreepUO2: provides thermal and irradiation creep
- RelocationUO2: provides burnup dependent relocation, with a relocation activation power of 5 kW/m
- Sifgrs: provides mechanistic fission gas release calculation

Since the case 1 model did not include cladding, no cladding irradiation growth, cladding thermal, or cladding solid mechanics material models were included. For the case 2 series, the clad material had a constant thermal conductivity of 16 W/m-K was used and both thermal (primary and secondary) and irradiation creep were considered.

G.3.3. Input files

The BISON input and all supporting files (power histories, axial power profile, mesh input, etc.) for this case are provided with the code distribution at bison/assessment/FUMEXII_simplified_cases/analysis.

G.3.4. Execution Summary

Assessment cases are ran nightly with the most recent version of the code. Table G.4 summarizes the date and version of the code used to generate results shown in this document.

Table G.4.: Execution summary.

Experiment	Machine	Operating System	Code Version
27(1)	Mac Workstation	OS X	BISON 1.0
27(2a)	Mac Workstation	OS X	BISON 1.0
27(2b)	Mac Workstation	OS X	BISON 1.0
27(2c)	Mac Workstation	OS X	BISON 1.0
27(2d)	Mac Workstation	OS X	BISON 1.0

G.4. Results Comparison

G.4.1. Fission Gas Release

As mentioned above, the Vitanza criteria is an empirical relationship derived from operational data at the Halden reactor. The empirical relationship has the form

$$T_{CL} = \frac{9800}{\ln\left(\frac{Bu}{0.005}\right)} \quad (G.1)$$

where T_{CL} is the fuel pellet centerline temperature in C and Bu is the burnup in MWd/kgUO₂. Equation G.1 provides the locus of centerline temperature-Bu pairs at the onset of fission gas release (onset taken to be approximately 1% FGR) for Halden operational history (e.g. various LHR with standard BWR flow, pressure, and fluid temperature values). The computational process described above was implemented with BISON to determine the onset of 1% FGR for several different LHR. Table G.5 shows BISON numerical results for linear heat rates ranging from 15 to 45 kW/m.

Table G.5.: BISON fuel centerline temperature versus burnup at onset of FGR (various linear heat rates) for the simplified case FUMEXII 27(1).

Burnup (MWd/kgU)	FCT (C)	LHR (kW/m)
78.8	960.1	20.0
48.8	1036.6	25.0
32.6	1096.6	30.0
21.8	1150.4	35.0
13.9	1201.0	40.0
7.8	1249.2	45.0

The BISON predictions and other code comparisons (data digitized from FUMEX-II report [19]) are shown with the Vitanza Criteria in Figure G.7.

The Vitanza criteria was derived from pressure, burnup, and centerline temperature data gathered during Halden reactor operations. Most of the experimental data base for the threshold development was for maximum Bu of about 40 MWd/kgU. Reference [19] suggests that the threshold may be somewhat conservative at higher burnups as recent high burnup data shows enhancement of FGR due to rim effect (enhanced porosity) development at the pellet surface. Several of the codes shown in Figure G.7 have FGR models that predict gas release to be independent of fuel temperature above some burnup limit. Predictions that become vertical are indicative of this feature. BISON results are generally in good agreement with the other code results though it is clear that considerable scatter exists among the predictions.

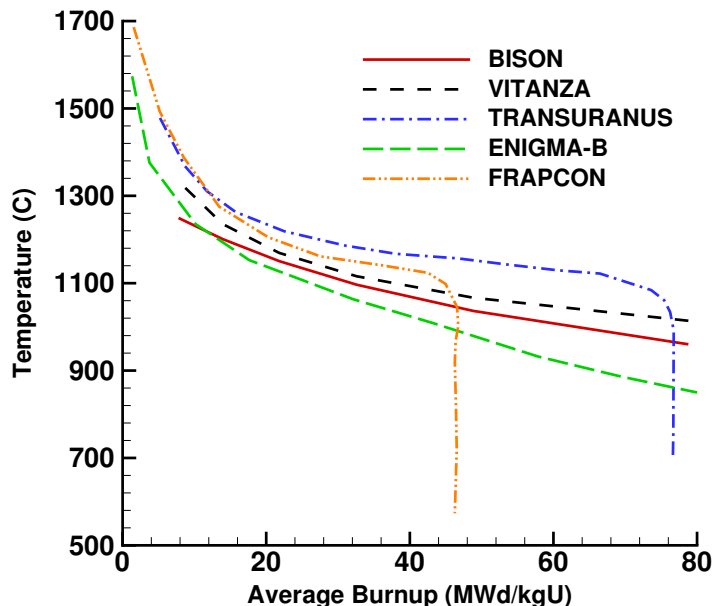


Figure G.7.: 27(1) BISON and other code results compared to Vitanza criteria [19].

BISON compares well with other well known fuel performance codes. All of the data for the other codes were digitized from plots in the FUMEX-II report [19]. Code comparisons for cases 27(2a) and 27(2b) are shown in Figure G.8 and Figure G.9, respectively.

BISON under predicts the total FGR at high burnup, but is within an acceptable range at low and moderate burnup. The BISON comparisons to other fuel performance codes for case 27(2c) are shown

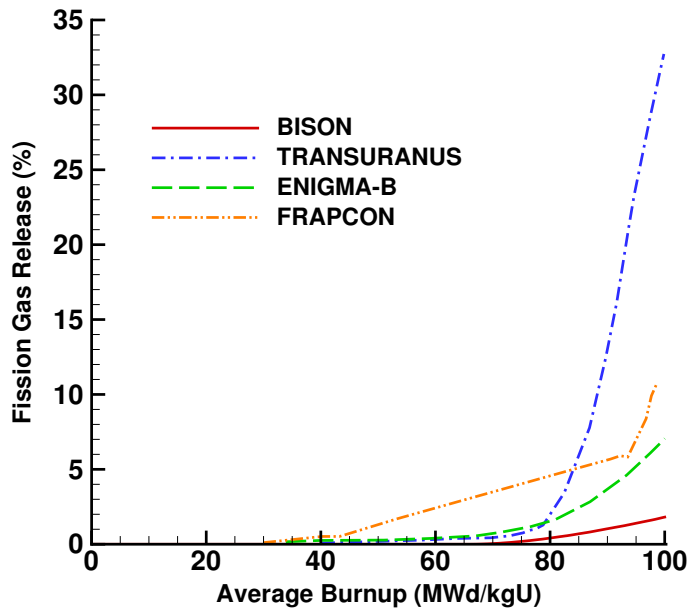


Figure G.8.: Case 27(2a) BISON comparisons with other well known fuel performance codes [19].

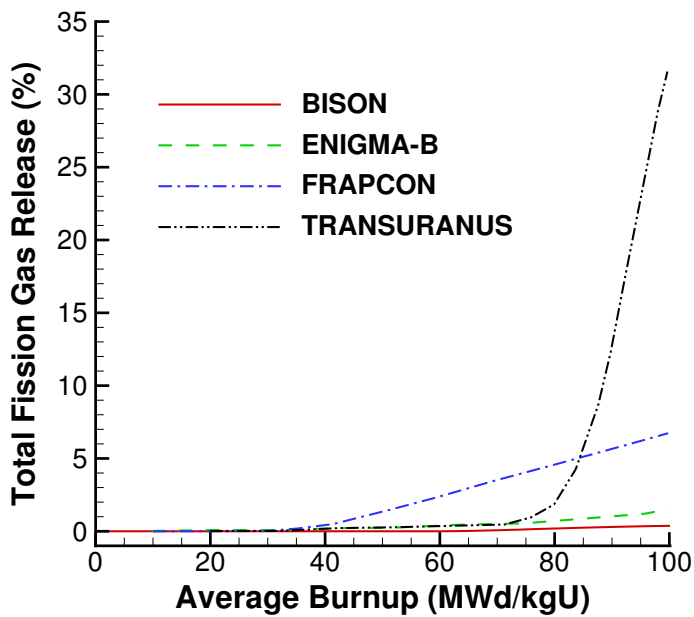


Figure G.9.: Case 27(2b) BISON comparisons with other well known fuel performance codes [19].

in Figure G.10. The BISON comparisons to expected FGR values and other fuel performance codes for case 27(2d) are shown in Figure G.11.

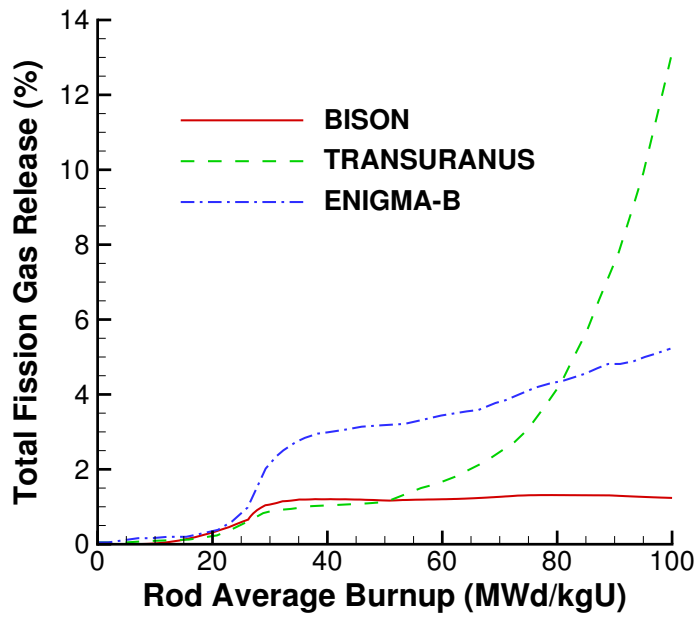


Figure G.10.: Case 27(2c) BISON comparisons with other well known fuel performance codes [19].

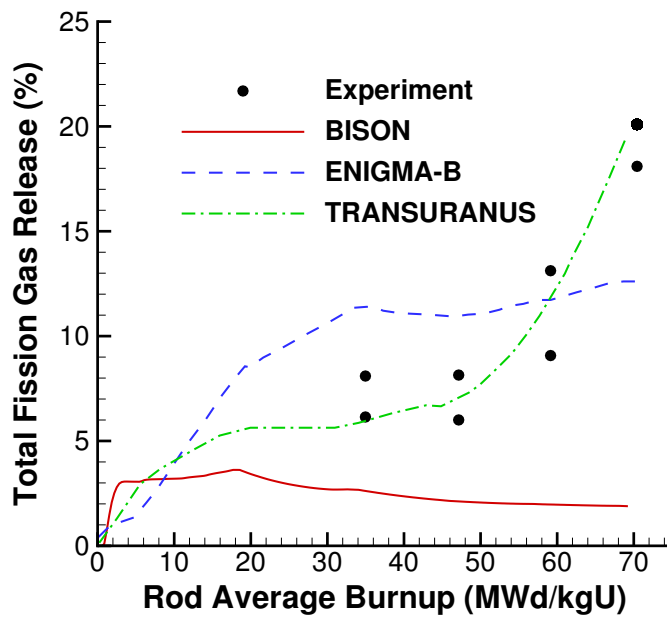


Figure G.11.: Case 27(2d) BISON comparisons with other well known fuel performance codes [19].

G.5. Discussion

As discussed above, the mesh shown in Figure G.3 includes only the fuel pellet. Specifications for FUMEXII 27(1) problem suggested that modelers use a large fuel rod plenum to preclude thermal feedback effects from the plenum and gap on FGR. After some experimentation with this concept, it became

apparent that in BISON it was computationally more efficient to eliminate the cladding and plenum altogether since unrestricted fission gas release was the matter of interest.

The overall results from the FUMEX-II simplified cases study indicate that a more accurate high burnup release model is needed in BISON. At low and moderate burnup, BISON does an adequate job predicting total fission gas release.

H. Risø GE7

H.1. Overview

The Risø-3 GE7 test is a bump test that was carried out during the third Risø Transient Fission Gas Release Project in 1989 [35]. The fuel pin ZX115 was supplied by General Electric Company and was neither punctured nor opened for re-fabrication prior the test. The test pin was the lower middle segment of four approximately 0.975 m long segments assembled to a stringer. The fuel segment was base irradiated in the Quad Cities-1 boiling water reactor (BWR) over four reactor cycles. The bump test was performed in the water-cooled HP-1 rig under BWR conditions in the DR3 test reactor.

H.2. Test Description

H.2.1. Rod Design Specifications

The rod specifications for the Risø-3 GE7 test is are summarized in Table H.1.

Table H.1.: Risø-3 GE7 rod specifications.

Fuel Rod		
Fuel stack height	m	0.7521
Nominal plenum height	mm	0.1445
Number of pellets per rod		72
Fill gas composition		He
Fill gas pressure	MPa	0.29
Fuel		
Material		UO ₂
Enrichment	%	3
Density	%	95.2
Outer diameter	mm	10.41
Pellet geometry		Chamfered
Grain diameter	μm	11.3-12.8
Pellet Chamfer (both ends)		
Dish diameter	cm	–
Dish depth	cm	–
Chamfer width	mm	0.18
Chamfer depth	mm	0.38
Cladding		
Material		Zr-2
Outer diameter	mm	12.26
Inner diameter	mm	10.63
Wall thickness	mm	0.815

H.2.2. Operating Conditions and Irradiation History

The base irradiation average power is shown in Figure H.1. The average power during the ramp test is shown in Figure H.2. The axial power profile is nearly linear for the base irradiation, however, during the ramp test, the power is shifted heavily to the bottom of the rod (see Figure H.3). The clad surface temperature was input as a function, along with the fast neutron flux from data provided in the FUMEX-III data set [33]. The coolant inlet temperature and pressure for the base irradiation and power ramp is shown in Table H.2.

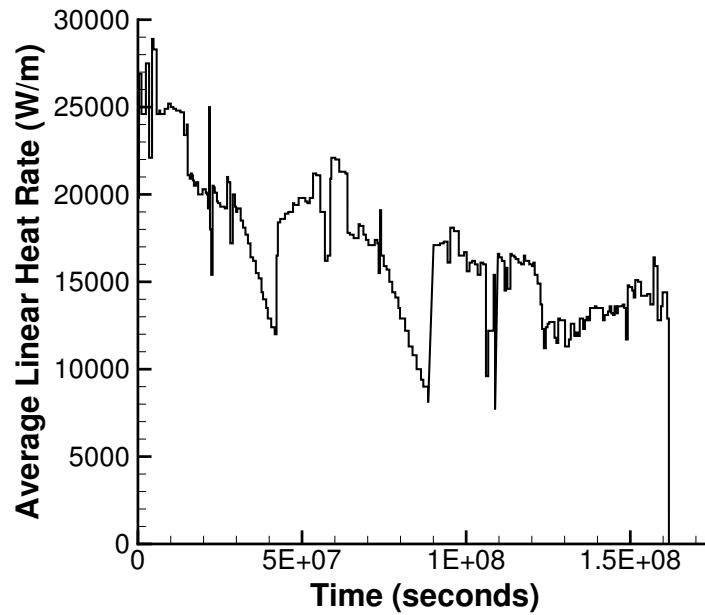


Figure H.1.: Base irradiation average power history for test pin ZX115.

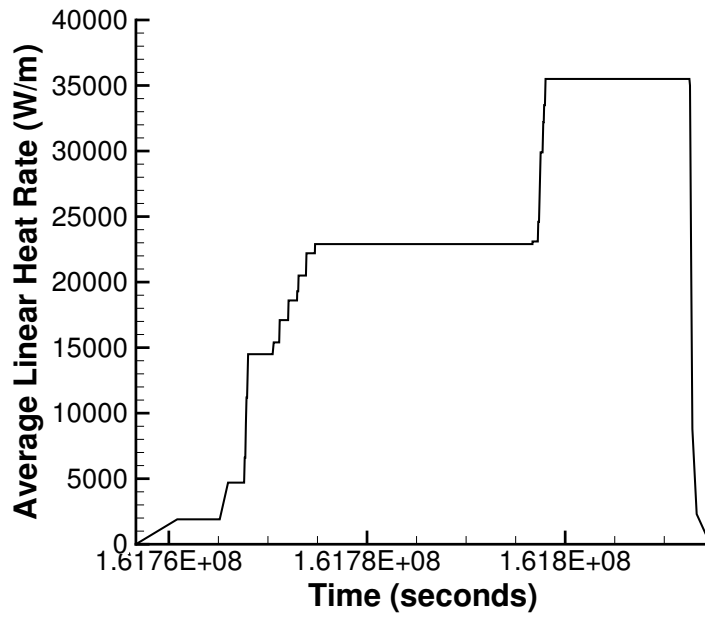


Figure H.2.: Average power history during power ramp.

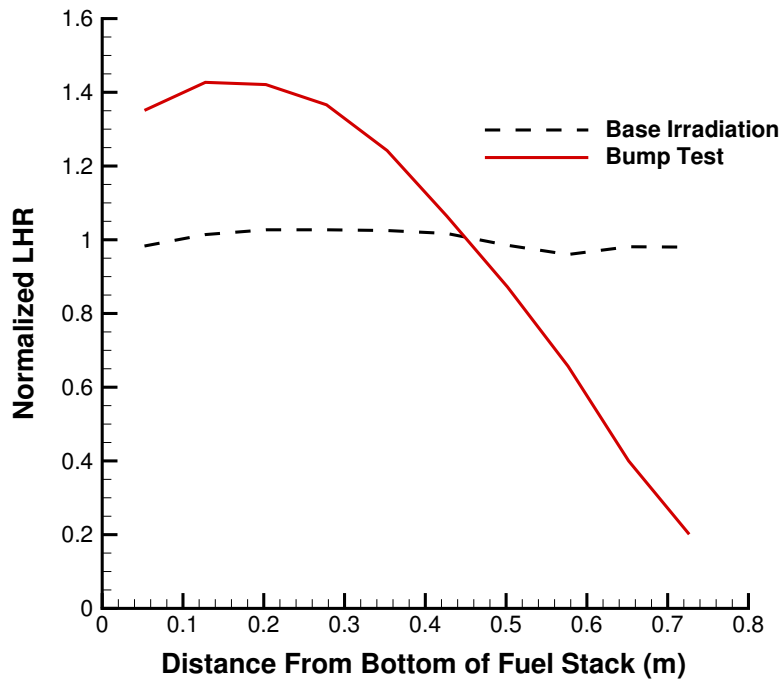


Figure H.3.: Axial power profile during base irradiation and ramp test.

Table H.2.: Operational input parameters.

Base Irradiation		
Coolant inlet temperature	C	295
Coolant pressure	MPa	7.24
Power Ramps		
Coolant inlet temperature	C	289
Coolant pressure	MPa	7.24

H.3. Model Description

H.3.1. Geometry and Mesh

The geometric parameters specified in Table H.1 were used to create the mesh for this simulation. The fuel was meshed as a single smeared fuel column with 11 radial elements and 432 axial elements. Figure H.4 shows a section of the mesh with a temperature contour plot.

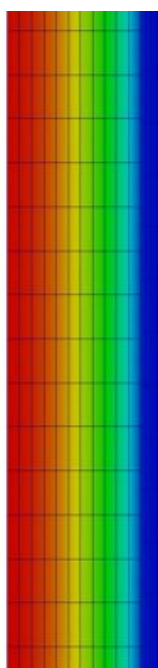


Figure H.4.: A section of the GE7 ZX115 fuel rod mesh with a temperature contour plot.

H.3.2. Material and Behavioral Models

The following material and behavioral models were used for the UO_2 fuel:

- ThermalFuel - NFIR: temperature and burnup dependent thermal properties.
- RelocationUO2: relocation strains, relocation activation threshold power set to 5 kW/m.
- Sifgr: Simplified fission gas release model with physics based gaseous swelling model.

For the clad material, a constant thermal conductivity of 16 W/m-K was used and both thermal (primary and secondary creep) and irradiation creep were considered.

H.3.3. Input files

The BISON input and all supporting files (power histories, axial power profile, fast neutron flux history, etc.) for this case are provided with the code distribution at bison/assessment/Riso_GE7_ZX115/analysis.

H.3.4. Execution Summary

Table H.3.: Execution summary.

Machine	Operating System	Code Version
Mac Workstation	OS X	BISON 1.0

H.4. Results Comparison

H.4.1. Clad Diameter

A comparison of the predicted and measured rod outer diameter is shown in Figure H.5. The solid green line is the as-manufactured rod diameter, prior to irradiation. The experimental data, as shown as “x” symbols, indicate the measured average rod diameter at both the end and middle fuel pellet locations, giving an indication of rod ridging due to pellet hour-glassing. The solid red line is the BISON predicted rod diameter following the power bump and the delta symbols indicate predicted rod diameter at the end pellet and mid pellet locations from the ENIGMA fuel performance code.

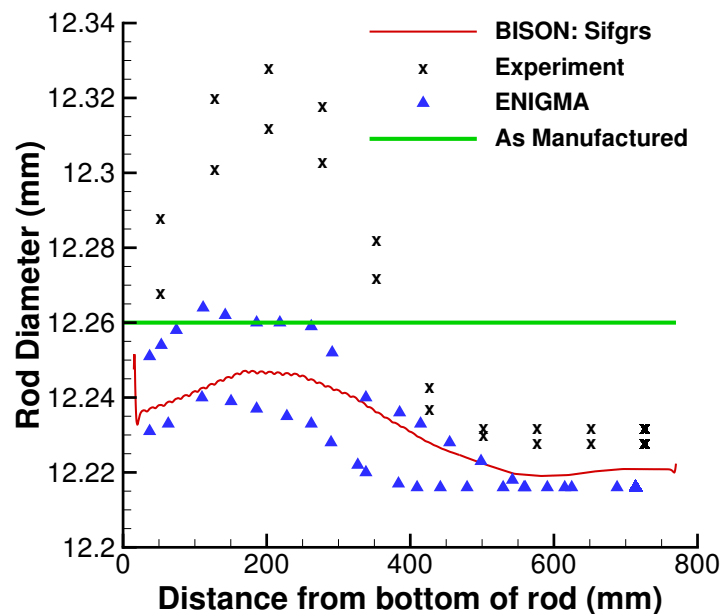


Figure H.5.: Risø GE7 experimental rod diameter comparisons after the power ramp. A comparison to the well known fuel performance code ENIGMA is also included in this plot.

H.4.2. Fission Gas Release

A comparison of the predicted and measured total fission gas release is shown in Figure H.6. BISON predicts the FGR well at the end of the base irradiation, however, at the end of the ramp test, BISON under predicts the total FGR.

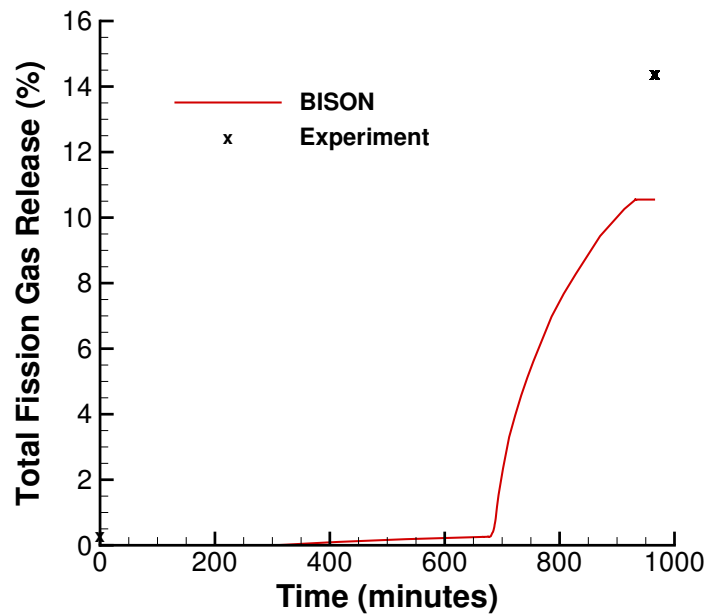


Figure H.6.: Risø GE7 experimental fission gas release comparisons after the power ramp.

H.5. Discussion

There are two swelling models within BISON. The primary swelling model is part of the fission gas release model, Sifgrs, which simulates swelling based on fission gas release. The other swelling model is empirical and referred to as VSwellingUO2. It was of interest to determine the difference between the swelling models. Figure H.7 shows the comparisons between the rod diameters from the different swelling models after the power ramp.

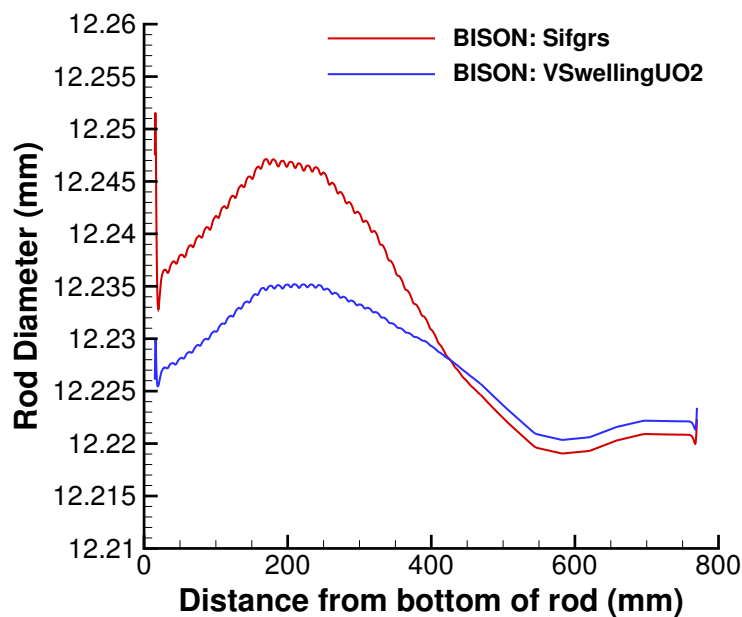


Figure H.7.: BISON swelling model comparisons of the final rod diameter at the end of the power ramp.

The calculation for the final rod diameter could be improved. The objective of future development activities is to combine primary and secondary creep models with an instantaneous plasticity model. Part of the development effort includes determining yield properties of zirconium alloy, which are functions of irradiation and temperature.

I. OSIRIS J12

I.1. Overview

This test is of a segmented PWR rod base-irradiated in the Electricity of France (EDF) Gravline 5 PWR [33]. The segment was then re-fabricated and ramp-tested in the French Alternative Energies and Atomic Energy Commission (CEA) OSIRIS reactor to investigate PCMI resistance. This experiment was chosen because it allows for an evaluation of several aspects of the code, including fully coupled thermo-mechanics, contact, and several nonlinear material models.

I.2. Test Description

I.2.1. Rod Design Specifications

The geometric input parameters for the OSIRIS J12 test are summarized in Table I.1.

Table I.1.: OSIRIS J12 Test Rod Specifications

Fuel Rod		
Overall length	m	0.5224
Fuel stack height	m	432.95
Nominal plenum height	mm	89.44
Number of pellets per rod		32
Fill gas composition		He
Fill gas pressure	MPa	2.6
Fuel		
Material		UO ₂
Enrichment	%	4.5
Density	%	95.73
Outer diameter	mm	8.192
Pellet geometry		Dished
Grain diameter	μm	10
Pellet Dishing (no chamfers)		
Dish diameter	mm	6
Dish depth	mm	0.32
Cladding		
Material		Zr-2
Outer diameter	mm	9.5
Inner diameter	mm	8.36
Wall thickness	mm	0.57

I.2.2. Operating Conditions and Irradiation History

The approximately 0.522 m segmented Zircaloy-4 clad rod was irradiated for 2 cycles in the EDF Gravline 5 PWR to a final discharge burn-up of 23.852 MWd/kgU. The average powers in the 2 cycles were approximately 16 and 23 kW/m. The rod segment designated J12-5, which was irradiated in the fifth span from the lower end of the assembly, was refabricated with new end plugs without altering either the fuel column or the internal fill gas. After a conditioning period of 762 minutes at 21 kW/m, the power was increased quickly (9 kW/m/min.) and held at 39.5 kW/m for 739 minutes. The axial profile was flat during base irradiation. The peaking factors during the bump test varied from approximately 0.75 at the ends of the segment to 1 at the center. The power history is presented in Figure I.1, and the power ramp is shown in Figure I.2. The initial fill-gas (Helium) pressure was 2.6 MPa, and the coolant pressure was 15.5 MPa. The external clad temperature was defined as a function of time and constant in space over the section of rod, the specified clad temperature in Figure I.3 was used in this simulation. The clad temperature was about 585 K during base irradiation and about 615 K during the ramp. The fast neutron flux in the clad was supplied via input using experimental data supplied with the experiment. Operational input parameters are summarized in Table I.2.

Table I.2.: Operational input parameters.

Base Irradiation		
Coolant inlet temperature	C	
Coolant pressure	MPa	15.5
Fast neutron flux	n/(m ² ·s) per (W/m)	4.8·10 ¹³
Power Ramp		
Coolant inlet temperature	C	
Coolant pressure	MPa	14.7
Fast neutron flux	n/(m ² ·s) per (W/m)	4.8·10 ¹³

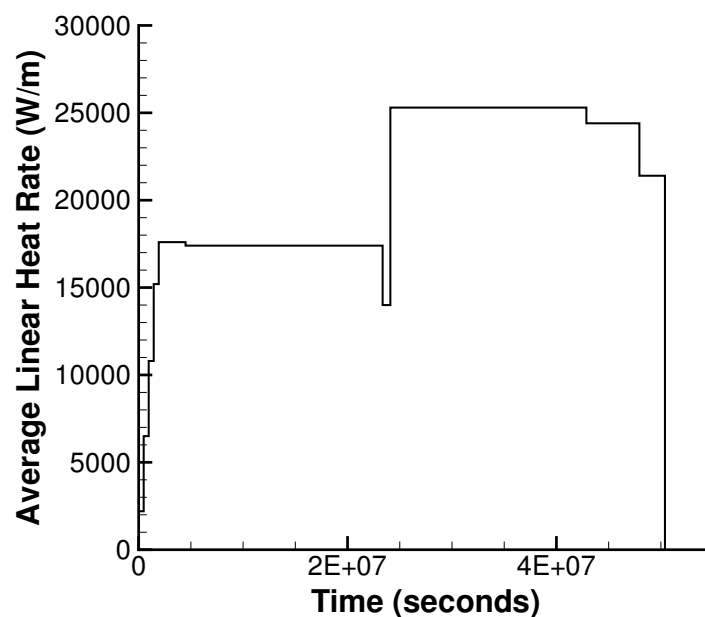


Figure I.1.: OSIRIS J12 power history in the Gravlines 5 PWR.

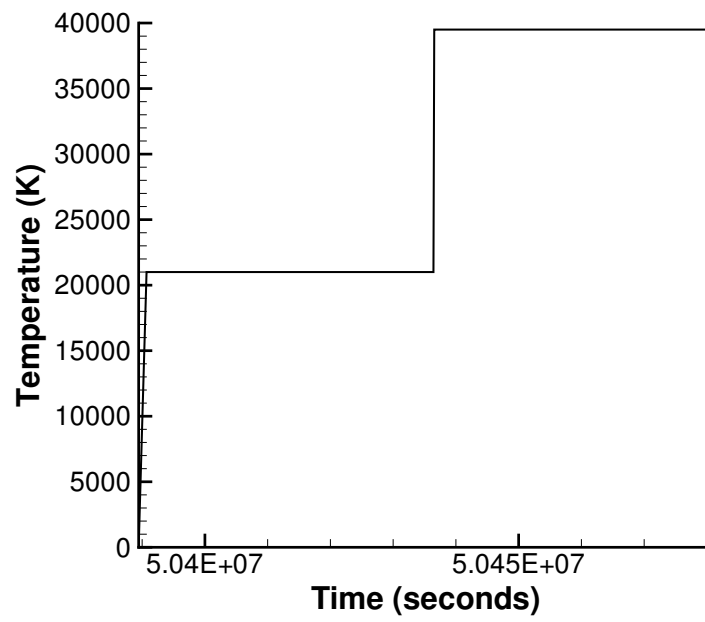


Figure I.2.: OSIRIS J12 power ramp

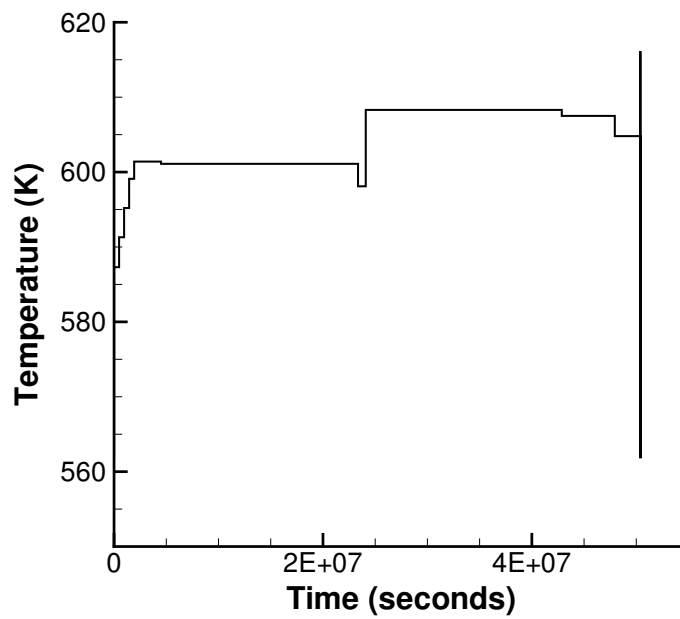


Figure I.3.: OSIRIS J12 clad temperature

I.3. Model Description

I.3.1. Geometry and Mesh

The rod specifications in Table I.1 were used as input for the geometry for this simulation. The J12-5 rod was modeled as a 2D-RZ axisymmetric discrete pellet mesh with quadratic elements. Each pellet consisted of 16 axial elements and 9 radial elements. The clad was meshed with 4 elements through the thickness. Figure I.4 is a section of the mesh with a temperature contour.

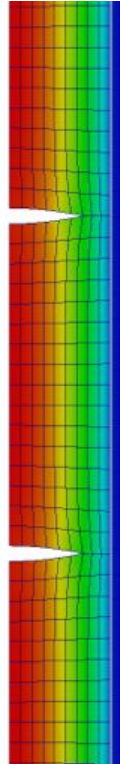


Figure I.4.: OSIRIS J12-5 mesh with temperature contour.

I.3.2. Material and Behavioral Models

The following material and behavioral models were used for the UO_2 fuel:

- ThermalFuel - NFIR: temperature and burnup dependent thermal properties
- RelocationUO2: relocation strains, relocation activation threshold power set to 5 kW/m.
- Sifgrs: Simplified fission gas release model with a combined solid/gaseous swelling model based on fission gas release.

For the clad material, a constant thermal conductivity of 16 W/m-K was used and both thermal (primary and secondary) and irradiation creep were considered.

I.3.3. Input files

The BISON input and all supporting files (power histories, axial power profile, fast neutron flux history, etc.) for this case are provided with the code distribution at `bison/assessment/OSIRIS_J12/analysis`.

I.3.4. Execution Summary

Table I.3.: Execution summary.

Machine	Operating System	Code Version
Mac Workstation	OS X	BISON 1.0

I.4. Results Comparison

I.4.1. Clad Diameter

A comparison of the predicted and measured rod outer diameter is shown in Figure I.5. The solid blue line is the as-manufactured rod diameter, prior to irradiation. The experimental data, shown as “+” (post-ramp) and “x” (pre-ramp) symbols, indicate the measured average rod diameter at both the end and middle fuel pellet locations, giving an indication of rod ridging due to pellet hour-glassing. The green solid line is the predicted rod diameter following the power bump and the red solid line is the predicted rod diameter prior to the ramp.

BISON under predicts clad creep down resulting in a larger than measured diameter. The overall shape of the rod after the ramp is captured well with BISON, as well as the clad ridging caused by the hour glassing (bamboo effect) of the discrete pellets.

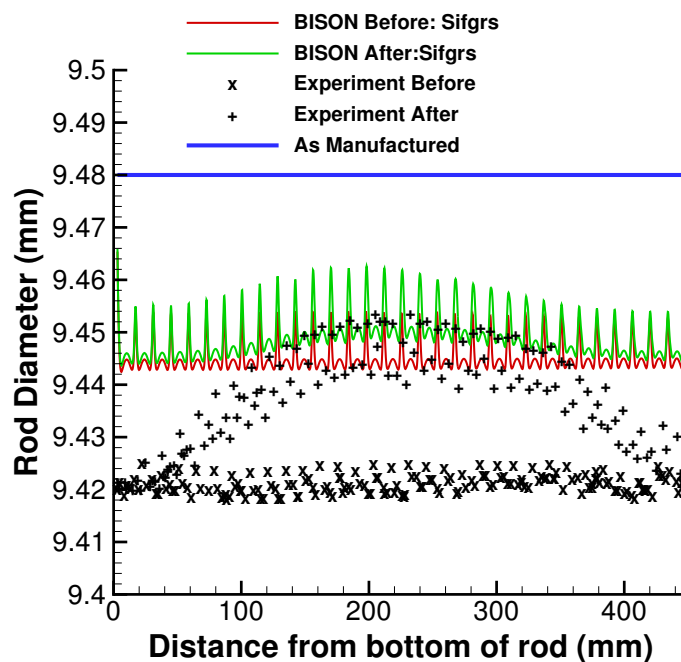


Figure I.5.: OSIRIS J12 experimental measurements and BISON calculation results from before and after the power ramp.

I.5. Discussion

There are two swelling models within BISON. The primary swelling model is part of the fission gas release model, Sifgrs, which simulates swelling based on fission gas release. The other swelling model is empirical [18] and referred to as VSwellingUO2. It was of interest to determine the difference between

the swelling models. Figure I.6 shows the comparisons between the rod diameters from the different swelling models from before and after the power ramp.

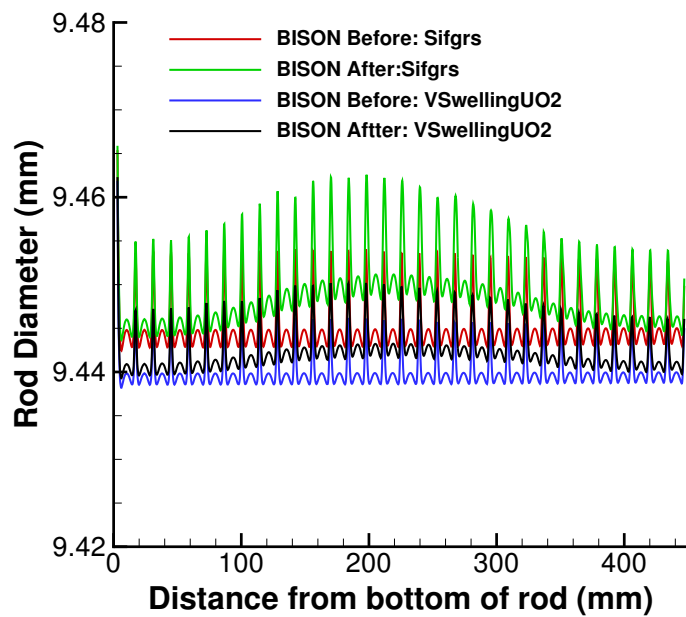


Figure I.6.: Effects of gaseous swelling model on BISON rod diameter predictions, before and after the power ramp.

The calculation for the final rod diameter could be improved. The objective of future development activities is to combine primary and secondary creep models with an instantaneous plasticity model. Part of the development effort includes determining yield properties of zirconium alloy, which are functions of irradiation and temperature.

J. REGATE

J.1. Overview

Regate is one of the experiments of the Fuel Modeling at Extended Burnup (FUMEX-II) program [19]. This experiment was carried out in order to provide data on Fission Gas Release (FGR) and clad diameter change. The rod is a short fuel segment irradiated in a commercial PWR and ramped in the french SILOE test reactor. The original segment was base irradiated in the Gravlines 5 PWR up to 47.415 MWd/kgHM.

Non-destructive post-irradiation examination (PIE) was performed on the fuel segment after discharge from the Gravlines 5 PWR with measurements on clad diameter and total fission gas release (based on Kr-85 gamma scan measurements), the total measured FGR after base irradiation was 1.5%. It is important to note that the fuel segment was not subject to any re-fabrication after base irradiation in Gravlines 5 PWR (power history shown in Figure J.1).

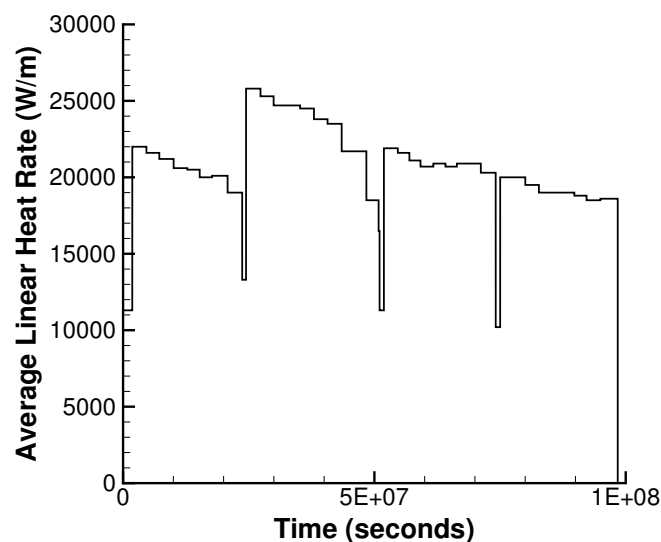


Figure J.1.: Rod average power history in the Gravlines 5 reactor.

The Kr-85 concentration was also measured with gamma scanning to measure a total of 9.3% FGR after the ramp test in the SILOE reactor. Puncturing tests were done after the power ramp in the SILOE reactor, to measure the total FGR of 10.2%. The oxide layer thickness and total clad diameter were also measured in PIE after the ramp test.

BISON comparisons to clad diameter and FGR are reported herein.

J.2. Test Description

J.2.1. Rod Design Specifications

The geometric input parameters for the FumexII–Regate case are summarized in Table J.1.

Table J.1.: Regate geometric input parameters

Fuel Rod		
Overall length	m	0.522
Fuel stack height	m	0.43595
Nominal plenum height	mm	48.15
Number of pellets per rod		32
Fill gas composition		He
Fill gas pressure	MPa	2.5
Fuel		
Material		UO ₂
Enrichment	%	4.487
Density	%	94.8
Outer diameter	mm	8.192
Pellet geometry		dished
Grain diameter	μm	8.7
Pellet Dishing		
Dish diameter	mm	6
Dish depth	mm	0.32
Chamfer width	mm	0.531
Chamfer depth	mm	0.16
Cladding		
Material		Zr-2
Outer diameter	mm	9.5
Inner diameter	mm	8.36
Wall thickness	mm	0.57

J.2.2. Operating Conditions and Irradiation History

The irradiation was adjusted by varying the distance of the rig from the SILOE core. The ramp test irradiation history consisted of a pre-condition power step of 19.5 kW/m (peak power) for 48 hours, prior to ramping at 1.0 kW/m/min up to 38.5 kW/m (peak power) which was held for 1.5 hours. The rod average power history during the SILOE irradiation is shown in Figure J.2. As the height of the SILOE reactor (~0.6 m) is comparable to the segment length (~0.44 m), the axial power is not flat during the ramp test, leading to values of $P_{average}/P_{max}$ of 0.9 and P_{min}/P_{max} of 0.65.

Table J.2.: Operational input parameters.

Base Irradiation		
Clad temperature	C	317
Coolant pressure	MPa	15.5
Fast neutron flux		Figure J.3
Power Ramps		
Clad temperature	C	77 -338
Coolant pressure	MPa	13
Fast neutron flux	n/(cm ² ·s)	2.0·10 ¹³

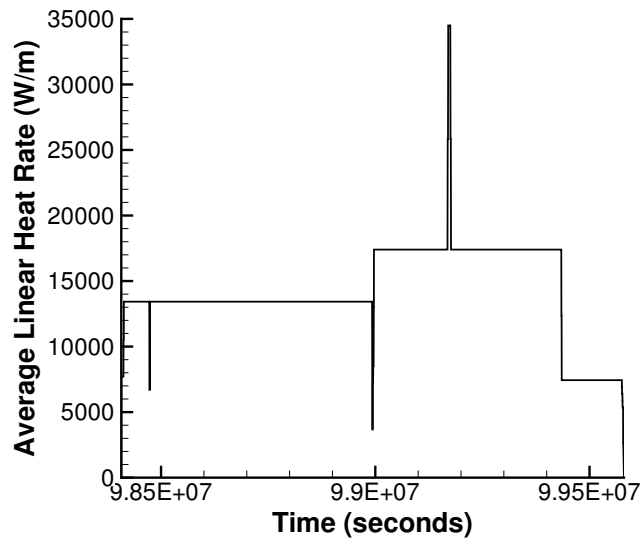


Figure J.2.: Rod average power history in the SILOE reactor.

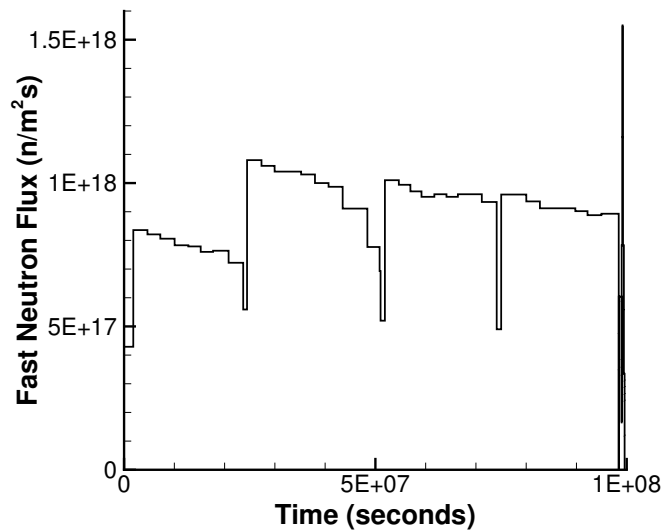


Figure J.3.: Fast neutron flux history. This history was supplied with the experimental data.

J.3. Model Description

J.3.1. Geometry and Mesh

A 2D-RZ axisymmetric discrete pellet mesh with quadratic elements was used to model this experiment. Each pellet was meshed with 16 axial and 9 radial elements. The clad was meshed with 4 axial elements. Figure J.4 shows a section of the meshed with a temperature contour plot during the ramp test.

J.3.2. Material and Behavioral Models

The following material and behavioral models were used for the UO₂ fuel:

- ThermalFuel - NFIR: temperature and burnup dependent thermal properties

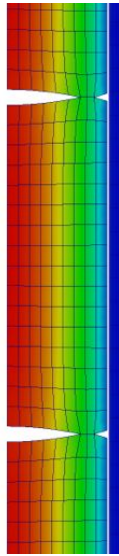


Figure J.4.: Section of mesh used for Regate simulation with temperature contour during the ramp test in the SILOE reactor.

- RelocationUO2: relocation strains, relocation activation threshold power set to 5 kW/m.
- Sifgrs: Simplified fission gas release model with a combined solid/gaseous swelling model based on fission gas release.

For the clad material, a constant thermal conductivity of 16 W/m-K was used and both thermal (primary and secondary) and irradiation creep were considered.

J.3.3. Input files

The BISON input and all supporting files (power histories, axial power profile, fast neutron flux history, etc.) for this case are provided with the code distribution at bison/assessment/FUMEXII_Regate/analysis.

J.3.4. Execution Summary

Table J.3.: Execution summary.

Machine	Operating System	Code Version
Mac Workstation	OS X	BISON 1.0

J.4. Results Comparison

J.4.1. Fission Gas Release

BISON over predicts FGR after the base irradiation in the Gravlines 5 PWR and under predicts the FGR at the end of the ramp test. The comparisons are plotted in Figure J.5.

J.4.2. Clad Diameter

BISON over predicts clad creep down which results in a smaller diameter than measured during PIE. The BISON comparisons to experimental measurements before and after the ramp are shown in Figure J.6.

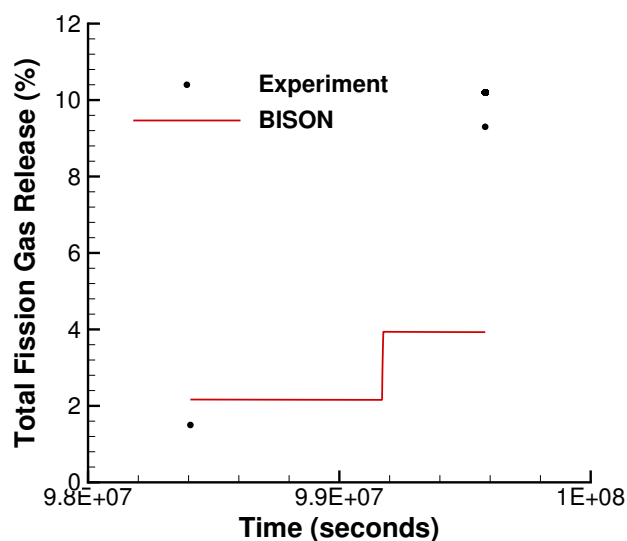


Figure J.5.: BISON FGR comparisons to experimental data.

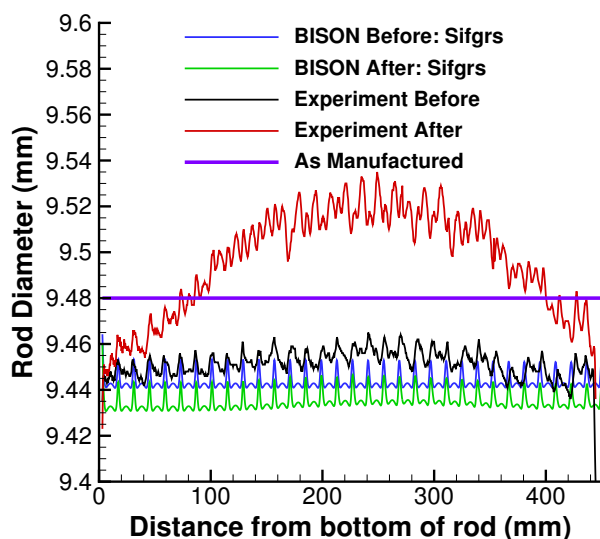


Figure J.6.: BISON rod diameter comparisons to experimental measurements before and after the power ramp.

J.5. Discussion

There are two swelling models within BISON. The primary swelling model is part of the fission gas release model, Sifgrs, which simulates swelling based on fission gas release. The other swelling model is empirical [18] and referred to as VSwellungUO2. It was of interest to determine the difference between the swelling models. Rod diameter calculations before and after the power ramp are shown in Figure J.7 for the different swelling models.

The calculation for the final rod diameter could be improved. The objective of future development activities is to combine primary and secondary creep models with an instantaneous plasticity model. Part of the development effort includes determining yield properties of zirconium alloy, which are functions of irradiation and temperature.

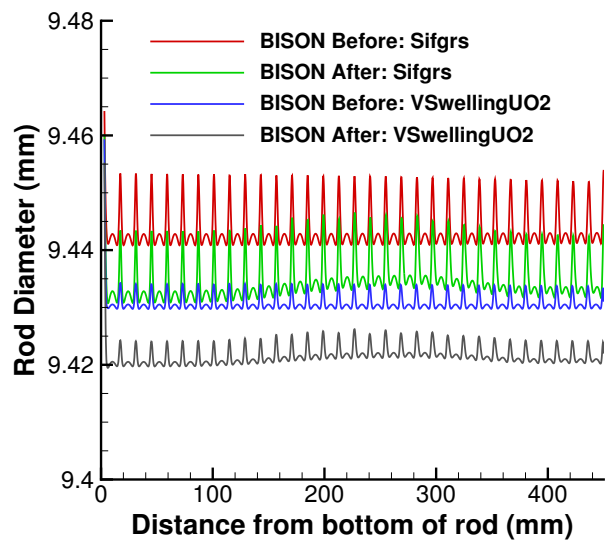


Figure J.7.: Effects of gaseous swelling model on BISON rod diameter predictions from before and after the power ramp.

Bibliography

- [1] R. L. Williamson, J. D. Hales, S. R. Novascone, M. R. Tonks, D. R. Gaston, C. J. Permann, D. Andrs, and R. C. Martineau. Multidimensional multiphysics simulation of nuclear fuel behavior. *J. Nuclear Materials*, 423:149–163, 2012.
- [2] J. D. Hales, R. L. Williamson, S. R. Novascone, D. M. Perez, B. W. Spencer, and G. Pastore. Multidimensional multiphysics simulation of TRISO particle fuel. *J. Nuclear Materials*, 443:531–543, 2013.
- [3] Pavel Medvedev. Fuel performance modeling results for representative FCRD irradiation experiments: Projected deformation in the annular AFC-3A U-10Zr fuel pins and comparison to alternative designs. Technical Report INL/EXT-12-27183 Revision 1, Idaho National Laboratory, 2012.
- [4] J. Killeen, E. Sartori, and T. Tverberg. FUMEX-III: A new IAEA coordinated research project on fuel modeling at extended burnup, paper 2176. In *Proceedings of Top Fuel 2009*, Paris, France, Sept 6-10, 2009.
- [5] J. C. Killeen, J. A. Turnbull, and E. Sartori. Fuel modelling at extended burnup: IAEA coordinated research project FUMEX-II. In *Proceedings of the 2007 International LWR Fuel Performance Meeting*, San Francisco, California, Paper 1102, September 30–October 3 2007.
- [6] Advances in high temperature gas cooled reactor fuel technology. Technical Report IAEA-TECDOC-1674, International Atomic Energy Agency, 2012.
- [7] J. D. Hales, S. R. Novascone, G. Pastore, D. M. Perez, B. W. Spencer, and R. L. Williamson. BISON theory manual: The equations behind nuclear fuel analysis. Technical report, Idaho National Laboratory, 2013.
- [8] J. D. Hales, S. R. Novascone, G. Pastore, D. M. Perez, B. W. Spencer, and R. L. Williamson. BISON users manual. Technical report, Idaho National Laboratory, 2013.
- [9] K. Lassman, C. O’Carroll, J. van de Laar, and C. T. Walker. The radial distribution of plutonium in high burnup UO₂ fuels. *J. Nucl. Materials*, 208:223–231, 1994.
- [10] J.B. Ainscough, B.W. Oldfield, and J.O. Ware. Isothermal grain growth kinetics in sintered UO₂ pellets. *J. Nucl. Mater.*, 49:117–128, 1973.
- [11] Y. Rashid, R. Dunham, and R. Montgomery. Fuel analysis and licensing code: FALCON MOD01. Technical Report EPRI 1011308, Electric Power Research Institute, December 2004.
- [12] A. M. Ross and R. L. Stoute. Heat transfer coefficient between UO₂ and Zircaloy-2. Technical Report AECL-1552, Atomic Energy of Canada Limited, 1962.
- [13] C. M. Allison and et al. SCDAP/RELAP5/MOD3.1 code manual volume IV: MATPRO. Technical Report NUREG/CR-6150, Idaho National Laboratory, 1993.
- [14] D. D. Lanning and C. R. Hann. Review of methods applicable to the calculation of gap conductance in zircaloy-clad uo2 fuel rods. Technical Report BWNL-1894, UC-78B, 1975.

- [15] A. Marion (NEI) letter dated June 13, 2006 to H. N. Berkow (USNRC/NRR). Safety Evaluation by the Office of Nuclear Reactor Regulation of Electric Power Research Institute (EPRI) Topical Report TR-1002865, Topical Report on Reactivity Initiated Accidents: Bases for RIA Fuel rod Failures and Core Coolability Criteria. <http://pbadupws.nrc.gov/docs/ML0616/ML061650107.pdf>, 2006.
- [16] G. Pastore, L. Luzzi, V. Di Marcello, and P. Van Uffelen. Physics-based modelling of fission gas swelling and release in UO_2 applied to integral fuel rod analysis. *Nuclear Engineering and Design*, 256:75–86, 2013.
- [17] G. Pastore, J. D. Hales, S. R. Novascone, D. M. Perez, B. W. Spencer, and R. L. Williamson. Analysis of fission gas release in LWR fuel using the BISON code. In *2013 LWR Fuel Performance Meeting – TopFuel*, Charlotte, NC, September 15–19 2013.
- [18] C. M. Allison, G. A. Berna, R. Chambers, E. W. Coryell, K. L. Davis, D. L. Hagrman, D. T. Hagrman, N. L. Hampton, J. K. Hohorst, R. E. Mason, M. L. McComas, K. A. McNeil, R. L. Miller, C. S. Olsen, G. A. Reymann, and L. J. Siefken. SCDAP/RELAP5/MOD3.1 code manual, volume IV: MATPRO—A library of materials properties for light-water-reactor accident analysis. Technical Report NUREG/CR-6150, EGG-2720, Idaho National Engineering Laboratory, 1993.
- [19] Fuel Modelling at Extended Burnup (FUMEX-II): Report of a coordinated research project. Technical Report IAEA-TECDPC-xxxx, IAEA, 2002-2007.
- [20] G. K. Miller, D. A. Petti, J. T. Maki, and D. L. Knudsen. PARFUME theory and model basis report. Technical Report INL/EXT-08-14497, Idaho National Laboratory, 2009.
- [21] M. Phelip, F. Michel, M. Pelletier, G. Degeneve, and P. Guillermier. The ATLAS HTR fuel simulation code objectives, description and first results. In *2nd International Topical Meeting on High Temperature Reactor Technology*, pages 1–10, Beijing, China, September 2004.
- [22] D. G. Martin. Considerations pertaining to the achievement of high burn-ups in htr fuel. *Nuclear Engineering and Design*, 213:241–258, 2002.
- [23] E. Proksch, A. Strigl, and H. Nabielek. Production of carbon monoxide during burn-up of UO_2 kerneled HTR fuel particles. *Journal of Nuclear Material*, 107:280–285, 1982.
- [24] E. R. Bradley, M. E. Cunningham, and D. D. Lanning. Final data report for the instrumented fuel assembly (IFA)-432. Technical Report NUREG/CR-2567, PNNL-4240, 1982.
- [25] C. R. Hann, D. D. Lanning, E. R. Bradley, R. K. Marshall, M. E. Cunningham, and R. E. Williford. Data Report for the NRC/PNL Halden Assembly IFA-432. Technical Report NUREG/CR-0560, PNL-2673, 1978.
- [26] Wolfgang Wiesenack, 2012. IFA-431 Rods 1, 2, and 3 Halden data.
- [27] L. P. Swiler, R. L. Williamson, and D. M. Perez. Calibration of a fuel relocation model in BISON. In *Proceedings of the International Conference on Mathematics and Computational Methods Applied to Nuclear Science and Engineering*, Sun Valley, Idaho, May 5-9, 2013.
- [28] Wolfgang Wiesenack, November 2012. IFA-432 Rods 1, 2, and 3 Halden data.
- [29] T. Tverberg, M. Amaya. Study of thermal behaviour of UO_2 and $(\text{U,Gd})\text{O}_2$ to high burnup (IFA-515). Technical Report HWR-671, Halden, February 2001.
- [30] M. Vankeerbergen. The Integral Fuel Rod Behaviour Test IFA-597.2: Pre-characterization and Analysis of measurements. Technical Report HWR-442, Halden, March 1996.

- [31] I. Matsson and J. A. Turnbull. The Integral fuel rod behaviour test IFA-597.3: Analysis of the Measurements. Technical Report HWR-543, Halden, January 1998.
- [32] The Third Risø Fission Gas Project: Bump Test AN3 (CB8-2R). Technical Report Risø-FGP3-AN3, Risø, September 1990.
- [33] Improvement of Computer Codes used for Fuel Behavior Simulation (FUMEX-III): Report of a coordinated research project (DRAFT). Technical Report IAEA-TECDOC-xxxx, IAEA, 2008-2012.
- [34] C. Vitanza, E. Kolstad, and U. Graziani. Fission gas release from UO₂ pellet fuel at high burnup. In *Proceedings of the American Nuclear Society Meeting on Light Water Reactor Fuel Performance*, page 361, Portland, Oregon, Apr 29 to May 3, 1979.
- [35] The Third Risø Fission Gas Project: Bump Test GE7 (ZX115). Technical Report Risø-FGP3-GE7, Risø, September 1990.